

BAW-10240(NP)
Revision 0

Incorporation of M5™ Properties in Framatome ANP Approved Methods

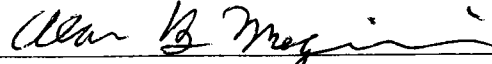
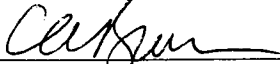


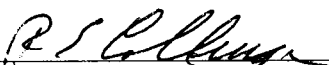
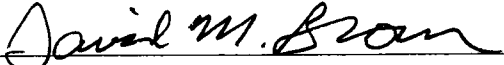
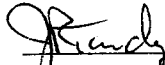

October 2002

Framatome ANP, Inc.

ISSUED IN FRA-ANP ON-LINE
DOCUMENT SYSTEM
DATE: 10-01-02

BAW-10240(NP)
Revision 0

**Incorporation of M5 Properties in
Framatome ANP Approved Methods**

Prepared:	<u></u>	<u>9/26/02</u>
	A. B. Meginnis, Engineer Safety Analysis Methods	Date
Prepared:	<u></u>	<u>9-26-02</u>
	C. A. Brown, Team Leader, Mech. Analysis Methods Product Mechanical Engineering	Date
Approved:	<u></u>	<u>9/27/02</u>
	D. W. Pruitt, Manager Safety Analysis Methods	Date
Approved:	<u></u>	<u>9/26/02</u>
	J. J. Cudlin, Manager Analysis Services	Date
Approved:	<u></u>	<u>9/27/02</u>
	R. E. Collingham, Manager BWR Reload Engineering & Methods Development	Date
Approved:	<u></u>	<u>9/28/02</u>
	D. M. Brown, Manager PWR Core Engineering	Date
Approved:	<u></u>	<u>26 Sept 02</u>
	J. R. Tandy, Manager Product Mechanical Engineering	Date
Approved:	<u></u>	<u>9/29/02</u>
	J. F. Mallay, Director Regulatory Affairs	Date

jrs

Customer Disclaimer

Important Notice Regarding the Contents and Use of This Document

Please Read Carefully

Framatome ANP, Inc.'s warranties and representations concerning the subject matter of this document are those set forth in the agreement between Framatome ANP, Inc. and the Customer pursuant to which this document is issued. Accordingly, except as otherwise expressly provided in such agreement, neither Framatome ANP, Inc. nor any person acting on its behalf:

- a. makes any warranty or representation, express or implied, with respect to the accuracy, completeness, or usefulness of the information contained in this document, or that the use of any information, apparatus, method, or process disclosed in this document will not infringe privately owned rights;
- or
- b. assumes any liabilities with respect to the use of, or for damages resulting from the use of, any information, apparatus, method, or process disclosed in this document.

The information contained herein is for the sole use of the Customer.

In order to avoid impairment of rights of Framatome ANP, Inc. in patents or inventions which may be included in the information contained in this document, the recipient, by its acceptance of this document, agrees not to publish or make public use (in the patent use of the term) of such information until so authorized in writing by Framatome ANP, Inc. or until after six (6) months following termination or expiration of the aforesaid Agreement and any extension thereof, unless expressly provided in the Agreement. No rights or licenses in or to any patents are implied by the furnishing of this document.

Nature of Changes

<u>Item</u>	<u>Paragraph or Page(s)</u>	<u>Description and Justification</u>
1.	All	This is a new document.

Contents

1.0	Introduction	1-1
2.0	Summary	2-1
2.1	Mechanical Methodology	2-1
2.2	SBLOCA Methodology	2-1
2.3	Non-LOCA Methodology	2-1
3.0	Methodology Overview	3-1
3.1	Mechanical Methodology	3-1
3.2	SBLOCA Methodology	3-1
3.3	Non-LOCA Methodology	3-2
3.4	Summary of Topical Reports	3-2
4.0	Incorporation of M5 Cladding Properties in RODEX2-2A	4-1
4.1	Summary of Cladding-Related Models in the Fuel Performance Evaluation Model	4-1
4.1.1	M5 Cladding Creep Correlation	4-1
4.1.2	M5 Cladding Free Growth Correlation	4-3
4.1.3	M5 Cladding Thermal Conductivity	4-4
4.1.4	M5 Cladding Zirconium Oxide Thermal Conductivity	4-4
4.1.5	M5 Cladding Specific Heat	4-4
4.1.6	M5 Cladding Density	4-4
4.1.7	M5 Cladding Thermal Expansion	4-5
4.1.8	M5 Cladding Elastic Modulus	4-6
4.1.9	M5 Cladding Poisson's Ratio	4-6
4.1.10	M5 Cladding Emissivity	4-6
4.1.11	M5 Cladding Corrosion	4-7
4.1.12	M5 Cladding Hydrogen Pickup	4-8
4.1.13	High Temperature M5/Steam Reaction Kinetics	4-8
4.1.14	M5 Cladding Swelling and Rupture/Blockage	4-9
4.2	Creep Parameters	4-9
4.2.1	Creep Benchmark Procedure	4-9
4.2.2	Creep Benchmark Results	4-10
4.3	Growth Benchmark Calculation for RODEX2-2A	4-10
5.0	Incorporation of M5 Properties in S-RELAP5	5-1
5.1	Summary of Cladding Related Models in the Thermal-Hydraulic Performance Evaluation Model	5-1
5.1.1	M5 Cladding Creep Correlation	5-1
5.1.2	M5 Cladding Free Growth Correlation	5-1
5.1.3	M5 Cladding Thermal Conductivity	5-1
5.1.4	M5 Cladding Oxide Thermal Conductivity	5-1
5.1.5	M5 Cladding Specific Heat	5-1
5.1.6	M5 Cladding Density	5-2
5.1.7	M5 Cladding Thermal Expansion	5-2
5.1.8	M5 Cladding Elastic Modulus	5-2
5.1.9	M5 Cladding Poisson's Ratio	5-3

5.1.10	M5 Cladding Emissivity	5-3
5.1.11	M5 Cladding Corrosion	5-3
5.1.12	M5 Cladding Hydrogen Pickup	5-3
5.1.13	High Temperature M5/Steam Reaction Kinetics	5-4
5.1.14	M5 Cladding Swelling and Rupture/Blockage	5-4
5.1.14.1	M5 Cladding Radial Ballooning and Rupture Deformations	5-4
5.1.14.2	Channel Flow Area and Flow Evaluations	5-7
6.0	PWR Mechanical Analysis Methodology	6-1
6.1	Fuel System Damage	6-1
6.1.1	Stress	6-1
6.1.2	Strain (RODEX2-2A)	6-2
6.1.3	Strain Fatigue (RAMPEX)	6-3
6.1.4	Fretting Wear	6-4
6.1.5	Oxidation, Hydriding, and Crud	6-4
6.1.6	Rod Bow	6-5
6.1.7	Axial Growth	6-6
6.1.7.1	Fuel Rod Growth	6-6
6.1.7.2	Fuel Assembly Growth	6-7
6.1.8	Rod Internal Pressure	6-6
6.1.9	Assembly Liftoff	6-9
6.1.10	Fuel Assembly Handling	6-9
6.1.11	Control Rod Reactivity	6-10
6.2	Fuel Rod Failure	6-10
6.2.1	Hydriding (Internal)	6-10
6.2.2	Cladding Collapse	6-11
6.2.3	Overheating of Cladding	6-13
6.2.3.1	Effect of M5 Cladding on DNB Phenomena	6-13
6.2.3.2	Effect of M5 Cladding on DNBR Criterion	6-13
6.2.4	Overheating of Fuel Pellets	6-14
6.2.5	Pellet-Cladding Interaction	6-14
6.2.6	Cladding Rupture	6-15
6.2.7	Mechanical Fracturing	6-15
6.3	M5 Sample Fuel Rod Analysis	6-16
6.3.1	Summary of Sample M5 Rod Analysis	6-16
6.3.2	Assembly Design	6-16
6.3.3	Rod Mechanical Evaluation	6-16
7.0	S-RELAP5 Based Appendix K PWR SBLOCA Methodology	7-1
7.1	Methodology Summary	7-1
7.2	Summary of Clad Related Models in the SBLOCA Methodology	7-2
7.2.1	RODEX2-2A	7-2
7.2.2	S-RELAP5	7-3
7.3	M5 Properties and Correlations Implemented in SBLOCA Models	7-3
7.3.1	Cladding Creep Correlation	7-3
7.3.2	Cladding Free Growth	7-3
7.3.3	Cladding Thermal Conductivity	7-4
7.3.4	Cladding Oxide Thermal Conductivity	7-4

7.3.5	Cladding Specific Heat.....	7-4
7.3.6	Cladding Density.....	7-4
7.3.7	Cladding Thermal Expansion.....	7-4
7.3.8	Cladding Modulus of Elasticity.....	7-4
7.3.9	Poisson's Ratio.....	7-5
7.3.10	Cladding Emissivity.....	7-5
7.3.11	Cladding Corrosion.....	7-5
7.3.12	Cladding Hydrogen Pickup.....	7-5
7.3.13	High Temperature M5/Steam Reaction Kinetics.....	7-6
7.3.14	Cladding Surface Roughness.....	7-6
7.3.15	Cladding Swelling and Rupture/Blockage.....	7-6
7.4	SBLOCA Sample Problem with M5 Cladding.....	7-6
8.0	Non-LOCA Methodology.....	8-1
8.1	Methodology Summary.....	8-1
8.1.1	SRP Chapter 15 Non-LOCA Transient Methodology.....	8-1
8.1.2	Statistical Setpoint/Transient Methodology for Westinghouse Type Reactors.....	8-2
8.1.3	Statistical Setpoint/Transient Methodology for Combustion Engineering Type Reactors.....	8-2
8.2	Summary of Clad Related Models in Non-LOCA Methodology.....	8-3
8.2.1	RODEX2-2A.....	8-3
8.2.2	S-RELAP5.....	8-3
8.3	M5 Properties and Correlations Implemented in Non-LOCA Models.....	8-4
8.3.1	Cladding Creep Correlation.....	8-4
8.3.2	Cladding Free Growth.....	8-4
8.3.3	Cladding Thermal Conductivity.....	8-5
8.3.4	Cladding Oxide Thermal Conductivity.....	8-5
8.3.5	Cladding Specific Heat.....	8-5
8.3.6	Cladding Density.....	8-5
8.3.7	Cladding Thermal Expansion.....	8-5
8.3.8	Cladding Modulus of Elasticity.....	8-5
8.3.9	Poisson's Ratio.....	8-6
8.3.10	Cladding Emissivity.....	8-6
8.3.11	Cladding Corrosion.....	8-6
8.3.12	Cladding Hydrogen Pick-up.....	8-6
8.3.13	Cladding Surface Roughness.....	8-6
8.4	M5 Setpoint Methodology Sample Problem.....	8-7
9.0	References.....	9-1

Tables

4.1	M5 Creep Benchmark Rods	4-11
4.2	Benchmark Rod Design Parameters	4-11
4.3	M5 Radial Creep Benchmark Results	4-12
5.1	Comparison of Young's Modulus for M5 and Zircaloy Cladding	5-10
5.2	M5 Cladding Rupture Strain	5-11
5.3	M5 Cladding Pre-Rupture Strain	5-12
5.4	M5 Cladding Assembly Blockage Fraction	5-13
5.5	Unblocked Flow Fraction	5-14
6.1	Fuel Assembly and Rod Description	6-18
6.2	Reactor Operating Conditions for Mechanical Evaluation	6-19
6.3	Design Duty Cycles for Cyclic Fatigue Evaluation	6-20
6.4	Mechanical Fuel Design Evaluation Results	6-21
6.5	Clad Stress Intensity Results	6-24

Figures

4.1	Integral Thermal Expansion for M5 Cladding	4-13
4.2	Emissivity of Non-Oxidized Samples Between 100°C and 400°C	4-14
4.3	Internal Emissivity of M5 Cladding	4-15
4.4	Calculated M5 Cladding Radial Creep Compared to Measured Creep	4-16
4.5	Calculated and Measured Radial Creep vs. Local Burnup	4-17
4.6	Comparison of Calculated Rod Growth to Measurements for Rod Specific Histories (1 st Part Validation Results)	4-18
4.7	Comparison of Calculated Rod Growth with Generic Histories to Ranges of Measured Data (2 nd Part Validation Results)	4-19
5.1	M5 Slow and Fast Heating Ramp Rate Rupture Strain	5-15
5.2	M5 Slow and Fast Heating Ramp Rate Pre-Rupture Strain	5-15
5.3	M5 Slow and Fast Heating Ramp Rate Assembly Blockage	5-16
6.1	M5 Fuel Rod Growth	6-25
6.2	M5 Assembly Growth	6-26
6.3	Comparison of COLAPX M5 Cladding Creep Model Calculated Radial Creep to Measured	6-27
6.4	COLAPX M5 Creep Model - Calculated Radial Creep and Measured vs. Local Burnup	6-28
6.5	Fuel Rod Power History Inputs For Limiting Cases - Rod Average LHGR	6-29
6.6	Fuel Rod Power History Inputs For Limiting Cases - Peak Rod Nodal LHGR	6-30
6.7	Predicted Maximum Fuel Rod Oxidation	6-31
6.8	Calculated Rod Internal Pressure versus Exposure	6-32
7.1	M5 PCT and Zircaloy PCT for the Limiting PCT Calculation (2-inch Break)	7-9
7.2	M5 PCT and Zircaloy PCT for the High Power 2-Inch Break	7-9

Nomenclature

<u>Acronym</u>	<u>Definition</u>
ASME	American Society of Mechanical Engineers
BOL	Beginning-of-life
BWR	Boiling water reactor
CE	Combustion Engineering
CEA	Commissariat à l'Énergie Atomique (French Atomic Energy Commission)
CFR	Code of Federal Regulations
CINOG	CINétique d'Oxydation à Grenoble
CWSR	Cold worked stress relieved
DNB	Departure from nucleate boiling
DNBR	Departure from nucleate boiling ratio
ECCS	Emergency core cooling system
EOL	End-of-life
FRA-ANP	Framatome ANP, Inc.
FTG	Framatome Technologies Group
HTP	High thermal performance
LBLOCA	Large break loss-of-coolant accident
LOCA	Loss-of-coolant accident
LTL	Lower tolerance limit
LTP	Lower tie plate
NRC	U.S. Nuclear Regulatory Commission
PCI	Pellet-clad interaction
PCT	Peak cladding temperature
PWR	Pressurized water reactor
S-RELAP5	Reactor leak and analysis safety program (code)
SBLOCA	Small break loss-of-coolant accident
SER	Safety Evaluation Report
SRP	Standard Review Plan
UTL	Upper tolerance limit
WREM	Water reactor evaluation model

1.0 Introduction

This report describes the incorporation of the U.S. Nuclear Regulatory Commission (NRC) approved M5®* material properties (References 1 and 2) into a set of Framatome ANP, Inc. (FRA-ANP) approved mechanical analysis, small break loss-of-coolant accident (SBLOCA), and non-loss-of-coolant accident (non-LOCA) methodologies. The mechanical analysis methodology is summarized in Reference 3, the SBLOCA methodology in Reference 4, and the non-LOCA methodologies in References 5, 6, and 7. This set of methodologies will be referred to as FRA-ANP Group M methodology to differentiate it from other FRA-ANP methods which have been approved by the NRC.

For most M5 material properties, an approved model from References 1 or 2 was available and incorporation of these properties into the methods was straightforward. However, some properties that were needed were either not available in the approved documents, required a range of applicability that extended outside the approved range, or required a new correlation for model-specific usage. These properties include creep, growth, thermal expansion, emissivity, elastic modulus, and rod rupture flow blockage.

Both the approved RODEX2-2A (Section 4.0) code and the S-RELAP5 (Section 5.0) code required modifications to integrate the approved M5 cladding material properties into the FRA-ANP methodologies. Some M5 material properties were available in a form that was more detailed than the current Zircaloy representation. As a result, some M5 cladding properties have been incorporated using a more detailed representation than was previously used for Zircaloy cladding.

No modifications to the base methodology were required for the inclusion of the M5 properties in the RODEX2-2A and S-RELAP5 codes. Modification of some of the approved mechanical criteria was required for consistency with the methodology approvals for M5. These include the clad stress limits and the clad corrosion criteria.

* M5 is a registered trademark of Framatome ANP, Inc.

M5 is a proprietary variant of Zr1Nb that has desirable high burnup performance. It provides significant improvements in corrosion, hydrogen pickup, axial growth and diametral creep relative to Zircaloy. Updates of M5 fuel rod and assembly growth measurements since the approval of the M5 topical report (Reference 1) are included.

2.0 **Summary**

2.1 ***Mechanical Methodology***

The implementation of the M5 properties in the RODEX2-2A code is described, followed by a description of the incorporation of the M5 properties into the evaluation of each of the Standard Review Plan (SRP) evaluation criteria, and finally a sample analysis of an M5 fuel rod in a Zircaloy-4 fuel assembly cage is presented.

2.2 ***SBLOCA Methodology***

The implementation of M5 properties in the RODEX2-2A and S-RELAP5 codes is described. A description of the incorporation of the M5 properties into the approved FRA-ANP Group M SBLOCA evaluation model is then given, followed by a sample SBLOCA analysis with Zircaloy-4 and M5 fuel rods.

2.3 ***Non-LOCA Methodology***

The implementation of M5 properties in the RODEX2-2A and S-RELAP5 codes is described. A description of the incorporation of the M5 properties into the approved FRA-ANP Group M SRP Chapter 15 non-LOCA evaluation model is then given. Additionally, a description of the incorporation of the M5 properties into the approved statistical setpoint methodology for both Westinghouse and Combustion Engineering (CE) PWRs is presented with a Zircaloy-4 and M5 comparative test case.

3.0 **Methodology Overview**

3.1 ***Mechanical Methodology***

The FRA-ANP Group M mechanical analysis methodology for pressurized water reactors (PWR) is defined by generic criteria (Reference 3), and by the generic methodology (References 8 through 15), which is summarized and referenced in the generic criteria report with the exception of Reference 15.

For the implementation of M5 cladding, M5 guide tubes, and M5 grid spacers, FRA-ANP uses the approved Group M evaluation methodology, but replaces the Zircaloy-4 material properties and correlations with the approved M5 properties and correlations (References 1 and 2). The implementation thus primarily addresses:

1. The incorporation of the M5 cladding properties (References 1 and 2) into the RODEX2-2A fuel performance code.
2. The incorporation of M5 cladding and guide tube growth correlations into bundle growth evaluations. Measurement data updates are included.
3. The incorporation of M5 modulus, thermal expansion, density, and strength properties into the fuel rod and fuel assembly stress evaluation methodology.

The generic criteria (Reference 3) are revised for the cladding maximum stress. The maximum stress criteria, which are based on allowable yield and ultimate tensile strengths per the ASME Section III criteria, are revised consistent with the approved M5 topical (Reference 1) to utilize the circumferential yield strength of the M5 cladding in the allowable stress evaluation.

3.2 ***SBLOCA Methodology***

The FRA-ANP Group M Appendix K SBLOCA evaluation methodology for PWRs is defined by Reference 4 and is approved to satisfy the regulations for emergency core cooling system (ECCS) analyses given in 10CFR Part 50 Section 50.46 and Appendix K.

FRA-ANP's implementation of M5 cladding in the SBLOCA methodology uses the approved evaluation methodology of Reference 4 and adds the approved M5 properties and correlations (References 1 and 2) for M5 analyses. The implementation thus primarily addresses:

1. The incorporation of the M5 cladding properties (References 1 and 2) into the RODEX2-2A fuel performance code.
2. The incorporation of M5 cladding properties (References 1 and 2) into the S-RELAP5 thermal-hydraulic system and fuel response evaluation code.

Modification of the approved methodology beyond the addition of M5 specific material properties and models is not necessary.

3.3 **Non-LOCA Methodology**

Reference 5 defines the approved FRA-ANP Group M SRP Chapter 15 non-LOCA evaluation methodology for PWRs. The FRA-ANP Group M approved statistical setpoint methodology is defined by References 6 and 7.

FRA-ANP's implementation of M5 cladding in the non-LOCA methodologies uses the approved evaluation methodologies defined in References 5, 6, and 7, but substitutes the approved M5 specific properties (Reference 1 and 2) for the Zircaloy-4 material properties when M5 clad fuel is analyzed. The implementation thus primarily addresses:

1. The incorporation of the M5 cladding properties (References 1 and 2) into the RODEX2-2A fuel performance code.
2. The incorporation of M5 cladding properties (References 1 and 2) into the S-RELAP5 thermal-hydraulic system evaluation code and code input.

Modification of the approved methodologies beyond the use of M5 specific material properties and models is not necessary.

3.4 **Summary of Topical Reports**

A summary of relevant FRA-ANP Group M approved topical reports is provided. The report listing is arranged by methodology. The listing discusses how each report is affected by the incorporation of M5 cladding properties and models. A brief summary is then given on how each affected methodology is impacted by the incorporation of M5 cladding.

Fuel Performance Code

- XN-NF-81-58(P)(A) Revision 2 and Supplements 1 and 2, *RODEX2 Fuel Rod Thermal-Mechanical Response Evaluation Model*, Exxon Nuclear Company, March 1984.
- ANF-81-58(P)(A) Revision 2 Supplements 3 and 4, *RODEX2 Fuel Rod Thermal-Mechanical Response Evaluation Model*, Advanced Nuclear Fuels Corporation, June 1990.

These two topical reports (References 8 and 9) define the fuel performance code. This fuel performance code is used for mechanical analysis, centerline melt calculations for SRP Chapter 15 event analysis, and stored energy calculations for Appendix K large and small break

analyses. The incorporation of M5 cladding requires the addition of M5 specific properties to the RODEX2-2A code for analyses of mechanical performance, LOCA, and non-LOCA events.

The changes to the fuel performance code to model the M5 cladding are described in Section 4.0.

Mechanical Design Methodology

- XN-NF-82-06(P)(A) Revision 1 and Supplements 2, 4 and 5, *Qualification of Exxon Nuclear Fuel for Extended Burnup*, Exxon Nuclear Company, October 1986.
- ANF-88-133(P)(A) and Supplement 1, *Qualification of Advanced Nuclear Fuels' PWR Design Methodology for Rod Burnups of 62 GWd/MTU*, Advanced Nuclear Fuels Corporation, December 1991.

These topical reports (References 10 and 11) describe the mechanical design methodology.

The reports describe mechanical analysis for the assembly as well as the fuel rod.

These methods utilize the RODEX2-2A, RAMPEX, and COLAPX codes which have been revised to incorporate M5 properties as described in Sections 4.0, 6.1.2, 6.1.3, 6.1.5, 6.1.8, 6.2.2, 6.2.4, and 6.2.5.

The methods also utilize strength properties which have been revised to incorporate M5 strength properties as discussed in Sections 6.1.1 and 6.2.7, to incorporate M5 growth behavior as discussed in Sections 6.1.7 and 6.1.9, and to incorporate M5 stiffness and density as discussed in Section 6.2.7.

Fuel Rod Bow

- XN-75-32(P)(A) Supplements 1 through 4, *Computational Procedure for Evaluating Fuel Rod Bowing*, Exxon Nuclear Company, October 1983. [Base document not approved]

This topical (Reference 12) defines the fuel rod bow behavior that is used to evaluate the effect of rod bow on DNB margins. There is no change to the fuel rod bow model for the incorporation of M5 cladding and structural material, which is discussed in Section 6.1.6.

Gadolinia Fuel Properties

- XN-NF-79-56(P)(A) Revision 1 and Supplement 1, *Gadolinia Fuel Properties for LWR Fuel Safety Evaluation*, Exxon Nuclear Company, November 1981.
- XN-NF-85-92(P)(A), *Exxon Nuclear Uranium Dioxide/Gadolinia Irradiation Examination and Thermal Conductivity Results*, Exxon Nuclear Company, November 1986.

These two topical reports (References 16 and 17) define the gadolinia fuel properties.

The use of M5 cladding or structural material does not impact these two topicals.

Generic Design Criteria

- EMF-92-116(P)(A), *Generic Mechanical Design Criteria for PWR Fuel Design*, Siemens Power Corporation, February 1999.

This topical (Reference 3) describes the criteria by which fuel designs are evaluated. The criteria cover mechanical analysis, LOCA and non-LOCA analysis and neutronics analysis.

Changes are made to the generic design criteria for clad stress as described in Section 6.1.1 and for clad corrosion as described in Section 6.1.5 to evaluate the M5 cladding. There are no other criteria changes.

Neutronics

- EMF-96-029(P)(A) Volumes 1 and 2, *Reactor Analysis System for PWRs Volume 1 - Methodology Description, Volume 2 - Benchmarking Results*, Siemens Power Corporation, January 1997.

This topical (Reference 18) describes the neutronics analysis code system.

The use of M5 cladding or structural material does not impact this topical report.

Thermal Hydraulic/Mixed Core Analysis

- XN-NF-82-21(P)(A) Revision 1, *Application of Exxon Nuclear Company PWR Thermal Margin Methodology to Mixed Core Configurations*, Exxon Nuclear Company, September 1983.

This topical (Reference 19) describes how the thermal hydraulic code XCOBRA-IIIC is used to perform DNB calculations in a mixed core configuration.

The use of M5 cladding or structural material does not affect this topical report.

Non-LOCA Chapter 15 Event Analyses

- EMF-2310(P)(A) Revision 0, *SRP Chapter 15 Non-LOCA Methodology for Pressurized Water Reactors*, Framatome ANP, May 2001.

The following NRC approved documents are referenced in EMF-2310 (Reference 5). The documents may also be referenced by other documents but are listed here for convenience.

- XN-75-21(P)(A) Revision 2, *XCOBRA-IIIC: A Computer Code to Determine the Distribution of Coolant During Steady State and Transient Core Operation*, Exxon Nuclear Company, January 1986.
- XN-NF-78-44(NP)(A), *A Generic Analysis of the Control Rod Ejection Transient for Pressurized Water Reactors*, Exxon Nuclear Company, October 1983.

The topical report EMF-2310 and those reports it references (References 20 and 21) describe the non-LOCA methodology used to evaluate the SRP Chapter 15 non-LOCA events.

While differences between M5 and Zircaloy properties must be taken into consideration for SRP Chapter 15 non-LOCA event analyses, the possibility for a change in cladding type is specifically addressed in EMF-2310(P)(A). Therefore, the use of M5 cladding or structural material does not impact these topical reports. This methodology utilizes the RODEX2-2A and S-RELAP5 codes. Modifications associated with cladding type in these codes are discussed separately.

The requirements for SRP Chapter 15 non-LOCA analyses with M5 cladding are discussed in Section 8.0.

DNB Correlation

- EMF-92-153(P)(A) and Supplement 1, *HTP: Departure from Nucleate Boiling Correlation for High Thermal Performance Fuel*, Siemens Power Corporation, March 1994.

This topical report (Reference 22) describes the DNBR correlation used for the various Framatome PWR fuel designs.

The use of M5 cladding or structural material does not impact these topical reports.

Statistical Setpoint Methodology for Westinghouse Plant Types

- EMF-92-081(P)(A) Revision 1, *Statistical Setpoint/Transient Methodology for Westinghouse Type Reactors*, Siemens Power Corporation, February 2000.

This topical report (Reference 6) describes the statistical setpoint/transient methodology used to analyze Westinghouse type plants.

While the differences between M5 and Zircaloy material properties must be taken into consideration for the statistical setpoint/transient methodology, those issues are not specifically addressed by the above topical report. Instead, reference is made to the approved RODEX2-

2A code, which is described separately. Therefore, the use of M5 cladding or structural material does not affect this topical report. The changes to the RODEX2-2A code for the incorporation of M5 cladding are described in Section 4.0.

The impact of M5 properties on the statistical setpoint/transient methodology is discussed in Section 8.0

Statistical Setpoint Methodology for Combustion Engineering Plant Types

- EMF-1961(P)(A) Revision 0, *Statistical Setpoint/Transient Methodology for Combustion Engineering Type Reactors*, Siemens Power Corporation, July 2000.

This topical report (Reference 7) describes the statistical setpoint/transient methodology used to analyze Combustion Engineering type plants.

While the differences between M5 and Zircaloy material properties must be taken into consideration for the statistical setpoint/transient methodology, those issues are not specifically addressed by the above topical report. Instead, reference is made to the approved RODEX2-2A code, which is described separately. Therefore, the use of M5 cladding or structural material does not affect this topical report. The changes to the RODEX2-2A code for the incorporation of M5 cladding are described in Section 4.0.

The impact of M5 properties on the statistical setpoint/transient methodology is discussed in Section 8.0.

Appendix K Large Break LOCA Analyses

- EMF-2087(P)(A), SEM/PWR-98: ECCS Evaluation Model for PWR LBLOCA Applications, Siemens Power Corporation, June 1999.

The following NRC approved documents are referenced in EMF-2087 (Reference 23).

- XN-75-41(A) Volume 1, Volume II, Volume II Appendices, Volume III Revision 2, Supplements 1, 2, 3, 4, 5 Revision 1, 6 and 7, *Exxon Nuclear Company WREM-Based Generic PWR ECCS Evaluation Model*, Exxon Nuclear Company, February 1986.
- XN-76-27(A) and Supplements 1 and 2, *Exxon Nuclear Company WREM-Based Generic PWR ECCS Evaluation Model Update ENC-WREM-II*, Exxon Nuclear Company, March 1977.
- XN-76-44(A), *Revised Nucleate Boiling Lockout for ENC WREM-Based ECCS Evaluation Models*, Exxon Nuclear Company, February 1977.

- XN-CC-39(A) Revision 1, *ICECON: A Computer Program Used to Calculate Containment Back Pressure for LOCA Analysis Including Ice Condenser Plants*, Exxon Nuclear Company, October 1978.
- XN-NF-78-30(A) and Amendment 1, *Exxon Nuclear Company WREM-Based Generic PWR ECCS Evaluation Model Update ENC WREM-IIA Responses to NRC Request for Additional Information*, Exxon Nuclear Company, May 1979.
- XN-NF-82-20(P)(A) Revision 1 Supplement 2, *Exxon Nuclear Company Evaluation Model EXEM/PWR ECCS Model Updates*, Exxon Nuclear Company, February 1985.
- XN-NF-82-20(P)(A) Revision 1 and Supplements 1, 3 and 4, *Exxon Nuclear Company Evaluation Model EXEM/PWR ECCS Model Updates*, Advanced Nuclear Fuels Corporation, January 1990.
- XN-NF-82-20(P)(A) Revision 1 Supplement 6, *EXEM/PWR Large Break LOCA ECCS Model Updates*, June 1998.
- XN-NF-85-16(P)(A) Volume 1 and Supplements 1, 2 and 3; Volume 2, Revision 1 and Supplement 1, *PWR 17x17 Fuel Cooling Test Program*, Advanced Nuclear Fuels Corporation, February 1990.
- XN-NF-85-105(P)(A) and Supplement 1, *Scaling of FCTF Based Reflood Heat Transfer Correlation for Other Bundle Designs*, Advanced Nuclear Fuels Corporation, January 1990.

The topical report EMF-2087(P)(A) and the reports it references (References 24 through 33) describe the Appendix K PWR large break LOCA evaluation model. This evaluation model is not currently intended for use with M5 cladding and thus is not being revised by this topical report.

Small Break LOCA Analyses

- EMF-2328(P)(A) Revision 0, *PWR Small Break LOCA Evaluation Model, S-RELAP5 Based*, Framatome ANP, March 2001.

The following NRC approved document is referenced in EMF-2328 (Reference 4). The document may also be referenced by other documents but is listed here for convenience.

- XN-NF-82-07(P)(A) Revision 1, *Exxon Nuclear Company ECCS Cladding Swelling and Rupture Model*, Exxon Nuclear Company, November 1982.

The topical report EMF-2328(P)(A) and the reports it references (Reference 34) describe the S-RELAP5 based Appendix K PWR small break LOCA evaluation model.

The changes to the small break LOCA evaluation model to analyze M5 cladding and structural material are described in Section 7.0. The approved small break LOCA methodology utilizes the RODEX2-2A code to determine fuel rod material properties at the burnup of interest for the

initial fuel stored energy calculation and uses the S-RELAP5 code for the transient thermal hydraulic and fuel rod deformation response calculations. As a result, RODEX2-2A and S-RELAP5 require modifications to incorporate the M5 specific properties and models. The changes to the RODEX2-2A and S-RELAP5 codes for the incorporation of M5 cladding are described in Section 4.0 and 5.0, respectively.

Realistic LBLOCA

- EMF-2103(P), *Realistic Large Break LOCA Methodology for Pressurized Water Reactors*, Framatome ANP, Inc., Currently under Review by the NRC.
- ANF-90-145(P)(A) Volumes I and II and Supplement 1, *RODEX3 Fuel Rod Thermal-Mechanical Response Evaluation Model, Volume I Theoretical Model, Volume II Thermal and Gas Release Assessments*, Advanced Nuclear Fuels, April 1996.

The topical report EMF-2103 (Reference 35) describes the Realistic large break LOCA evaluation model. The use of M5 cladding is addressed in EMF-2103, including the modifications to the RODEX3 code (Reference 36).

Fuel Assembly Reconstitution

- ANF-90-82(P)(A) Revision 1 and Supplement 1, *Application of ANF Design Methodology for Fuel Assembly Reconstitution*, Siemens Power Corporation, May 1995.

This report (Reference 15) describes the application of the NRC approved design methodology to the evaluation of fuel assembly reconstitution.

The use of M5 cladding or structural material does not impact this topical report.

Power Distribution Control

- ANF-88-054(P)(A), *PDC-3 Advanced Nuclear Fuels Corporation Power Distribution Control for Pressurized Water Reactors and Application of PDC-3 to H. B. Robinson Unit 2*, Advanced Nuclear Fuels Corporation, October 1990.

This topical report (Reference 37) describes the power distribution control procedures used for Westinghouse type plants.

The use of M5 cladding or structural material does not affect this topical report.

Seismic

- XN-NF-696(P)(A), *ENC's Solution to the NRC Sample Problems-PWR Fuel Assemblies Mechanical Response to Seismic and LOCA Events*, Exxon Nuclear Company, April 1986.
- XN-76-47(P)(A), *Combined Seismic-LOCA Mechanical Evaluation for Exxon Nuclear 15x15 Reload Fuel for Westinghouse PWR's*, Exxon Nuclear Company, January 1982.

These reports (References 13 and 14) describe the seismic analysis methodology.

There are minor changes in stiffness and density parameters for these analyses described in Section 6.2.7. M5 material strengths are incorporated in the evaluation limits for M5 components. The use of M5 cladding or structural material does not affect the methodology of these topical reports.

Control Rod Worth Measurements

- XN-75-27(P)(A) Supplement 5, *Exxon Nuclear Neutronics Design Methods for Pressurized Water Reactors*, Exxon Nuclear Company, February 1987.

This report (Reference 38) describes a specific technique for measuring control rod worth during reactor startup physics tests.

The use of M5 cladding or structural material does not affect this topical report.

Kinetics Code

- XN-CC-32(P)(A), *XTRAN-PWR: A Computer Code for the Calculation of Rapid Transients in Pressurized Water Reactors with Moderator and Fuel Temperature Feedback*, Exxon Nuclear Company, September 1976.

This topical report (Reference 39) describes a two-dimensional kinetics code.

The use of M5 cladding or structural material does not affect this topical report.

Materials

- BAW-10227(P)(A), *Evaluation of Advanced Cladding and Structural Material (M5) in PWR Reactor Fuel*, Framatome Cogema Fuels, February 2000.

BAW-10227 is the main reference (Reference 1) for NRC-approved methodology for M5 cladding and structural material.

The properties described in BAW-10227 are being modified in the following areas in this report:

- Cladding creep
- Cladding growth
- Cladding thermal expansion
- Cladding emissivity
- Cladding elastic modulus
- Rod rupture flow blockage

The fuel rod and fuel assembly growth models are refined with the addition of more PIE data.

The modifications are described in Sections 4.0 and 5.0.

4.0 Incorporation of M5 Cladding Properties in RODEX2-2A

4.1 *Summary of Cladding-Related Models in the Fuel Performance Evaluation Model*

4.1.1 M5 Cladding Creep Correlation

Cladding creep is dependent on the stress history of the cladding wall, including the internal gas pressure, the coolant pressure, and the fuel cladding mechanical contact forces, as well as the temperature and irradiation histories. The creep model used in RODEX2-2A for M5 cladding is documented on Page G-10 of Reference 9 (MTYPE=4 Creep Model). The NRC has approved the use of the MTYPE=4 model in RODEX2-2A for SEM/PWR-98 application (Reference 23). This model was already available in RODEX2-2A. Only the constants have been adjusted to represent M5 cladding creep behavior as described in References 1 and 2. The previously defined M5 model for creep was not used in RODEX2-2A because the previously approved model (Reference 1) was not compatible with RODEX2-2A.

The generalized creep rate ($\dot{\epsilon}_c$, h^{-1}) is the sum of the thermal ($\dot{\epsilon}_p$, h^{-1}) and irradiation ($\dot{\epsilon}_i$, h^{-1}) components:

$$\dot{\epsilon}_c = \dot{\epsilon}_i + \dot{\epsilon}_p \quad 4.1$$

The thermal and irradiation creep component rates are evaluated using



The radial creep deformation is calculated in the same manner as for Zircaloy rods. [

] The radial creep deformation and axial creep strain at the end of a time step increment (Δt) are then given by:

4.2

4.3

The details of this process are described in Reference 8.

The values of the creep model constants used for M5 cladding are:

[] were calculated for M5 cladding based on creep anisotropy measurements. The value of [] was determined by benchmarking the overall RODEX2-2A creep model against M5 radial creep measurements from fuel irradiation test data. The results of the creep benchmarks are presented in Section 4.2.

4.1.2 M5 Cladding Free Growth Correlation

The M5 irradiation-induced cladding free growth contributes to the total fuel rod growth calculation in RODEX2-2A. Cladding free growth for M5 was not reported separately from total fuel rod growth in previously approved FRA-ANP submittals. For incorporation into RODEX2-2A, however, this model is described.

The irradiation-induced free growth of M5 is one part of the fuel rod elongation with the remainder coming from axial creep. The model, which is implemented in RODEX2-2A for irradiation-induced cladding free growth of M5, is a fraction of the existing Zircaloy-4 growth model. It was determined by benchmarking the overall rod elongation, including creep, against the irradiated M5 rod growth data. This benchmarking is described in Section 4.2.

The following lists the stress-free cladding growth model that generates good RODEX2-2A rod growth predictions for M5:

where

$\Delta L/L$ = elongation (%)
T = temperature (K)
 Φ = fast fluence (n/cm²)

4.1.3 M5 Cladding Thermal Conductivity

The thermal conductivity (W/m-K) of M5 cladding is taken from the NRC-approved Reference 2, Equation 10-30, and is described by the following equation:

4.4

where T is temperature (K). The equation applies to temperatures between [].

4.1.4 M5 Cladding Zirconium Oxide Thermal Conductivity

The Zirconia thermal conductivity values (W/m-K) on M5 cladding is taken from the NRC-approved Reference 2, Equations 10-31 through 10-33:

4.5

where S is the thickness (m) of the oxide layer and T is temperature (K). The thermal conductivity is dependent on the temperature and the thickness of the oxide layer.

4.1.5 M5 Cladding Specific Heat

Specific heat is not used in the RODEX2-2A code. RODEX2-2A calculations assume quasi-steady thermal conditions for each burnup interval so specific heat is not required.

4.1.6 M5 Cladding Density

Cladding density is not used in the RODEX2-2A code. Cladding density would be multiplied by specific heat to provide volumetric heat capacity. However, since RODEX2-2A assumes quasi-steady state heat transfer, volumetric heat capacity is not required.

4.1.7 M5 Cladding Thermal Expansion

The integral coefficient of thermal expansion is based on the model approved by the NRC in Reference 1, Appendix I and Section K-2.4. The α and β phase expansion rates were approved in Reference 1. Expansion rate coefficients for the current model follow those presented in References 1 and 2, except that the α phase expansion coefficient in the axial direction has been rounded down from [] to provide one value for the different components of an all M5 fuel assembly.

The safety evaluation report (SER) for Reference 1 states that the transition range in the approved model begins at a temperature that is about 60°C too low. In response to this observation, the transition region has been modified. For the $\alpha + \beta$ domain, the transition range will begin at []. The previous transition range was [].

As presented in Reference 1, Section K-2.4, it was determined that the relative contractions extrapolated to 850°C corresponding to $\alpha \rightarrow \beta$ phase transformation in the [] directions. These values allow calculation of the intersection with the Y-axis of the linear equation representing the β domain between []. The $\alpha + \beta$ thermal expansion equation is then obtained by constructing a linear connection between the α and β laws. Figure 4.1 presents the model from Reference 1, Appendix I, compared to the current model with the Reference 1, Section K-2.4 modification to relative contractions. The current model is defined as follows:

The thermal expansion strain (in/in) in the axial direction is represented by (assuming a reference temperature of 20°C):



4.6

The thermal expansion strain (in/in) in the tangential direction is represented by:



4.7

The thermal expansion strain (in/in) in the radial direction is represented by:

$$\epsilon_r = \alpha_r (T - T_0) \quad (4.8)$$

where T is temperature (°C).

Uncertainty in the α phase is []. Uncertainty is [] for the $\alpha \rightarrow \beta$ domain and for the β phase. Radial thermal expansion is associated with the change in thickness of the cladding due to thermal expansion and is only a small contributor to total thermal expansion in the radial direction; it is not considered in the approved RODEX2-2A cladding thermal expansion model. For RODEX2-2A, the low temperature range to 750°C is applicable.

4.1.8 M5 Cladding Elastic Modulus

The Young's modulus for cladding elastic deformation is taken from the NRC-approved Reference 2, Equation 10-54. The equation for Young's modulus (Pa) is as follows:

$$E = E_0 \left[1 - \frac{T - T_0}{T_1 - T_0} \right] \quad (4.9)$$

where T is cladding temperature (K).

Equation 4.9 is valid between [] with an uncertainty of [].

4.1.9 M5 Cladding Poisson's Ratio

Poisson's Ratio is taken from the NRC-approved Reference 1, Page I-75. As described in the reference, a [].

4.1.10 M5 Cladding Emissivity

Emissivity is used in the RODEX2-2A fuel model in calculating the small radiation component of the internal gap conductance. The emissivity correlation approved in Reference 1, Page I-73 is for high temperature oxidized applications []. RODEX2-2A calculations are typically performed at cladding temperatures below 400°C. At low temperatures and low oxidation, the emissivity of Zirconium alloys is smaller. The data produced by Murphy and Havelock (Reference 40) for Zr – 2.5% Nb alloy between 100°C and 400°C can be fitted by a degree 2 polynomial (Figure 4.2) to develop a low temperature, low oxidation correlation. To

provide a smooth transition between the high temperature and low temperature correlations, the range of the low temperature correlation is extended upward and the range of the high temperature correlation is extended downward to the crossover point of the two correlations

[]. The combined correlation over the entire temperature range can be seen in Figure 4.3.

Therefore, the emissivity (ϵ) for M5 is given by:

$$\left[\begin{array}{l} \text{Equation 4.10} \\ \text{Equation 4.11} \end{array} \right] \quad \text{and} \quad \left[\begin{array}{l} \text{Equation 4.10} \\ \text{Equation 4.11} \end{array} \right]$$

where T is temperature (°C).

For RODEX2-2A, the low temperature range to [] is applicable.

In case of a cladding temperature lower than [].

4.1.11 M5 Cladding Corrosion

The pre- and post-transition M5 cladding corrosion models presented in the NRC-approved Reference 2, Pages 8-7 through 8-9, and Equations 8-14 and 8-16 are implemented in RODEX2-2A. The pre-transition equation used in RODEX2-2A is []:

$$\left[\begin{array}{l} \text{Equation 4.12} \end{array} \right]$$

and the post-transition equation is:

$$\left[\begin{array}{l} \text{Equation 4.13} \end{array} \right]$$

where:

4.1.12 M5 Cladding Hydrogen Pickup

The M5 cladding relationship for hydrogen content presented in the NRC-approved Reference 2, Page 8-15, and Equation 8.37 is implemented in RODEX2-2A. This equation is as follows:

4.14

4.1.13 High Temperature M5/Steam Reaction Kinetics

The RODEX2-2A calculations are performed at normal reactor operating conditions. The temperature of the cladding during normal operating conditions is not high enough for significant metal-water reaction to take place. Therefore, only cladding corrosion models are used to determine cladding oxidation in the RODEX2-2A code. A separate high-temperature M5/steam reaction kinetics model is not required.

4.1.14 M5 Cladding Swelling and Rupture/Blockage

The RODEX2-2A code is used to calculate burnup dependent fuel behavior at normal reactor operating conditions. Under these conditions, swelling and rupture/blockage will not occur and, therefore, no swelling and rupture/blockage model is implemented in the RODEX2-2A code.

4.2 **Creep Parameters**

4.2.1 Creep Benchmark Procedure

Cladding creep is one of the most important M5 cladding properties incorporated into RODEX2-2A because of its difference from Zircaloy creep and its resultant impact on fuel rod thermal performance and temperature calculations. The previously defined M5 model for creep (Reference 1) was not used in RODEX2-2A because it was not compatible with RODEX2-2A. Therefore, it was necessary to benchmark the RODEX2-2A cladding creep model against radial creep measurements from M5 irradiation test data.

Data from [] M5 clad fuel rods were used to benchmark the radial cladding creep calculated by RODEX2-2A. The rods are listed in Table 4.1. Each of the rods has identical design parameters that are provided in Table 4.2.

The rods were irradiated in [

]. The radial creep was measured at 12 axial locations for each of the Cycle 1 and 2 rods, and at 10 axial locations for each of the Cycle 3 rods. These are the same rods referred to in Appendices I and J of Reference 1, and in Section 7 of Reference 2. The calculated burnups differ slightly from those reported in Reference 1 since the power history input used for RODEX2-2A was obtained independently.

The RODEX2-2A M5 creep parameters were established by regression analyses of the comparison of measured to calculated results for these rods for various creep coefficients. Regression analyses of the predicted one- and two-cycle creep versus the measured creep were used to select the parameters that produced results with a regression coefficient of 1.0.

The 3-cycle rod diameter measurement data were not included in regression analyses because the rod-diameter measurement results indicate that pellet-cladding interaction occurred during the third cycle of irradiation.

The RODEX2-2A parameter for ALM(1) was demonstrated to be the best-fit creep coefficient for RODEX2-2A M5 creep predictions at -53.52 with a regression constant of 0.99982.

4.2.2 Creep Benchmark Results

The radial cladding creep results calculated by RODEX2-2A are shown in Table 4.3, along with the measured values. Figure 4.4 also compares the calculated results to the measured values. Figure 4.5 compares the calculated and measured creep values as a function of local burnup. The figures demonstrate that the RODEX2-2A creep prediction gives acceptable agreement with the measured data.

4.3 ***Growth Benchmark Calculation for RODEX2-2A***

The M5 rod growth benchmarking indicated that the M5 stress-free irradiation growth coefficient differs from the one for Zircaloy. Also the application of friction force after pellet-clad interaction as described in the RODEX2-2A Equation G.7 of XN-NF-81-58(P)(A) is needed. The friction coefficient of 0.5 and the stress-free irradiation induced rod growth correlation for M5 cladding shown in Section 4.1.2 were determined through benchmarking to the rod growth results.

Post-irradiation measured M5 clad data were used for RODEX2-2A M5 rod growth validation. The M5 rod growth validation contains two parts. The first part is for the M5 rods that have had creep measured. The number of growth data points for these rods is limited, but rod-specific power histories are available. Figure 4.6 displays the first part validation results. The second part has a large number of M5 growth data points available, but no rod-specific power histories. Thus, typical 17x17 power histories were used for the validation. Figure 4.7 displays the second part validation results. Both Figures 4.6 and 4.7 demonstrate that the M5 rod growth models determined gave good growth predictions.

Table 4.1 M5 Creep Benchmark Rods



Table 4.2 Benchmark Rod Design Parameters



Table 4.3 M5 Radial Creep Benchmark Results



Figure 4.1 Integral Thermal Expansion for M5 Cladding

**Figure 4.2 Emissivity of Non-Oxidized Samples
Between 100°C and 400°C**



Figure 4.3 Internal Emissivity of M5 Cladding



**Figure 4.4 Calculated M5 Cladding Radial Creep
Compared to Measured Creep**

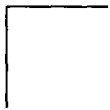


Figure 4.5 Calculated and Measured Radial Creep vs. Local Burnup



**Figure 4.6 Comparison of Calculated Rod Growth to Measurements
for Rod Specific Histories (1st Part Validation Results)**



Figure 4.7 Comparison of Calculated Rod Growth with Generic Histories to Ranges of Measured Data (2nd Part Validation Results)

5.0 Incorporation of M5 Properties in S-RELAP5

5.1 *Summary of Cladding Related Models in the Thermal-Hydraulic Performance Evaluation Model*

Currently, S-RELAP5 is approved for use in SBLOCA and SRP Chapter 15 non-LOCA calculations (References 4 and 5). For non-LOCA calculations, properties related to cladding and fuel-clad gap are input to the code, and the S-RELAP5 internal cladding models are not used. Therefore, the SBLOCA methodology is currently the only approved methodology that directly uses the cladding models in the S-RELAP5 code.

5.1.1 M5 Cladding Creep Correlation

Cladding creep is a burnup dependent parameter. The duration of an S-RELAP5 SBLOCA calculation is sufficiently short to hold burnup dependent parameters constant. Therefore, cladding creep is not calculated in the S-RELAP5 code.

5.1.2 M5 Cladding Free Growth Correlation

Cladding irradiation induced free growth is a burnup dependent parameter. The duration of an S-RELAP5 SBLOCA calculation is sufficiently short to hold burnup dependent parameters constant. Therefore, cladding free growth is not calculated in the S-RELAP5 code.

5.1.3 M5 Cladding Thermal Conductivity

The thermal conductivity model for M5 cladding described in Section 4.1.3 is also used in the S-RELAP5 code.

5.1.4 M5 Cladding Oxide Thermal Conductivity

The thermal conductivity model for M5 cladding oxide described in Section 4.1.4 is also used in the S-RELAP5 code.

5.1.5 M5 Cladding Specific Heat

The specific heat (J/kg-K) values for M5 cladding are approved in Reference 1, Page I-72 as follows:

5.1

The product of the density and the specific heat determines volumetric heat capacity.

5.1.6 M5 Cladding Density

The density of M5 cladding is taken from the NRC-approved Reference 1, Page I-70:

5.2

The density is used in the conduction equation to calculate the mass in the cell. Since the mass in a cell (mesh interval or node) and the cell dimensions do not change in the conduction solution scheme, the density used is that at room temperature. The use of temperature-dependent or phase-dependent density is not appropriate.

5.1.7 M5 Cladding Thermal Expansion

The thermal expansion model for M5 cladding described in Section 4.1.7 is also used in the S-RELAP5 code. For S-RELAP5, the models for the entire temperature range to 1400°C are incorporated.

5.1.8 M5 Cladding Elastic Modulus

The approved elastic modulus model for M5 cladding described in Section 4.1.8 is also used in the S-RELAP5 code. In S-RELAP5 applications, however, Equation 4.9 is assumed applicable to all temperatures of interest. Table 5.1 compares the elastic modulus values of M5 from Equation 4.9 and those for Zircaloy used in S-RELAP5/RODEX3A (Reference 41, Equation 7.127). The RODEX3A formulation is a more recent formulation from MATPRO-11 and provides a more detailed representation than that used for Zircaloy-4 in the SBLOCA methodology. The comparison shows that the extension of Equation 4.9 to the entire LOCA temperature range is within [] of the Zircaloy Young's modulus. This is within the standard error of the Zircaloy correlation (6400 MPa). Therefore, the range extension is acceptable.

5.1.9 M5 Cladding Poisson's Ratio

Poisson's Ratio for M5, [] described in Section 4.1.9, is also used in S-RELAP5.

5.1.10 M5 Cladding Emissivity

Emissivity is used in the RODEX2-2A fuel model in S-RELAP5 to calculate the radiation component of the internal gap conductance. For this purpose, S-RELAP5 uses the same values as described in Section 4.1.10. For S-RELAP5, the models for the entire temperature range to [] are incorporated. S-RELAP5 also calculates rod external radiation to the coolant. For this purpose, S-RELAP5 uses the emissivity defined in Section 4.8 of Reference 41. The value that is used is [] and is the same for both Zircaloy and M5 cladding. This value is based on the analysis of core cooling for BWR rod bundles. Using an external emissivity of [] is conservative relative to the recommended value for M5 of [] in Reference 1, Page I-73, and maintains consistency with the treatment of Zircaloy cladding. []

5.1.11 M5 Cladding Corrosion

Low temperature cladding corrosion is not calculated in S-RELAP5. The SBLOCA transient calculation performed by S-RELAP5 occurs over a short time period compared to the burnup calculation in RODEX2-2A and produces high-cladding temperatures. When high temperatures occur, corrosion is accelerated and the low temperature corrosion models are no longer valid. At the high cladding temperatures predicted in the S-RELAP5 calculation, a special high temperature M5/steam reaction kinetics model is needed. Section 5.1.13 describes the high temperature M5/steam reaction kinetics model used in S-RELAP5.

5.1.12 M5 Cladding Hydrogen Pickup

Cladding hydrogen pickup is not calculated in S-RELAP5. The cladding hydrogen pickup model described in Section 4.1.12 is associated with low temperature cladding corrosion. The SBLOCA transient calculation performed by S-RELAP5 produces high cladding temperatures where corrosion is accelerated and where the low temperature corrosion models are no longer valid. A special high-temperature M5/steam reaction kinetics model is then required as described in Section 5.1.13. Since the criteria for SBLOCA do not set limits on hydrogen pickup

but only on cladding oxidation, the high temperature M5/steam reaction kinetics model only considers oxidation and not hydrogen pickup.

5.1.13 High Temperature M5/Steam Reaction Kinetics

Metal-water reaction kinetics in S-RELAP5 for SBLOCA is calculated using the Baker-Just model (Reference 42) as described in Reference 41, Section 12.10. The same method is used for both Zircaloy and M5 cladding. Baker-Just was approved for use with M5 in Reference 1.

5.1.14 M5 Cladding Swelling and Rupture/Blockage

5.1.14.1 M5 Cladding Radial Ballooning and Rupture Deformations

The FRA-ANP M5 cladding ballooning and rupture model is used to compute the radial displacement due to cladding ballooning and rupture (Δr_{cr}) at each axial elevation as a function of the hoop stress (σ , kpsi), the average cladding temperature, and the dimensionless cladding heat-up rate (H_c). Cladding ballooning and/or rupture only occurs when the cladding temperatures are high and the inside rod pressure is greater than the pressure in the coolant channel. The hoop stress is given by the thin shell formula as described in Reference 41, Equation 12.26:

$$\sigma = 0.0005 \left(\frac{r_{co} + r_{ci}}{r_{co} - r_{ci}} \right) (P_{gap} - P_{cool}) \quad 5.3$$

where:

r_{co}	=	cladding outer radius (in)
r_{ci}	=	cladding inner radius (in)
P_{gap}	=	rod internal pressure (psi)
P_{cool}	=	rod external pressure (coolant channel pressure) (psi)

The cladding heat-up rate is based on the average cladding temperature, which is given by Reference 41, Equation 12.27:

$$\bar{T}_c = \frac{(T_{co} + T_{ci})}{2} \quad 5.4$$

where:

T_{ci}	=	cladding inner temperature (°F)
T_{co}	=	cladding outer temperature (°F)

The dimensionless cladding heat-up rate (H_c) is obtained by dividing the []
and limiting []

For M5 cladding, if the hoop stress is less than [], T_{rup} is set to the value predicted when the hoop stress is [] (Reference 1, Page K-24).

The cladding rupture temperature (T_{rup} , °C) or ($T_{rup,f}$, °F) for M5 cladding is computed by the following correlation (Reference 1, Page K-24):

$$T_{rup,f} = 1.8 T_{rup} + 32.0 \quad 5.5$$

where:

$$T_{rup,f} = 1.8 T_{rup} + 32.0 \quad 5.6$$

For [], [] is set to zero and no additional calculations are performed (Reference 43, Page 2.3-40).

If [], the cladding burst strains [] at temperature ramp rates of [] are obtained by linear interpolation of the rupture strain values in Table 5.2 (Reference 1, the strain function is plotted on Pages K-33 and K-34) which is plotted in Figure 5.1. Note that the approved table runs from []. It is anticipated that this range will span the range of temperatures at which rupture will occur. For completeness, however, the values at [] are programmed to be used for rupture temperatures below [], and the values at [] are programmed to be used for rupture temperatures above []. The cladding burst strain (ϵ_{cb}) is then obtained from one of the following relationships:

5.7

If [], the cladding hoop strain (ϵ_{cr}) equals the burst strain. If [] and [], the cladding pre-rupture hoop strains [] at temperature ramp rates of [] are obtained by linear interpolation of the pre-rupture strain values in Table 5.3 (Reference 1, the strain function is plotted on Pages K-33 and K-34) which is plotted in Figure 5.2. Note that the approved table runs from []. It is anticipated that this range will span the range of temperatures at which rupture will occur. For completeness, however, the values at [] are programmed to be used for rupture temperatures below [] and the values at [] are programmed to be used for rupture temperatures above []. The cladding pre-rupture hoop strain (ϵ_{cr}^p) is then obtained from one of the following relationships:

5.8

The cladding hoop strain (ϵ_{cr}) is then given by the following relationship (Reference 43, Page 2.3-41):

5.9

which [

], respectively. Finally, the deformation resulting from the cladding hoop strain is given by (Equation 12.33 of Reference 41):

5.10

5.1.14.2 Channel Flow Area and Flow Evaluations

Before the rupture of the fuel rod, the area of the channel around the fuel rod (A^f) is given by the following relationship (Equation 12.71 of Reference 41):

$$A^f = \text{Pitch}^2 - \pi \left(\frac{d}{2} \right)^2 \quad 5.11$$

where:

Pitch = the assembly's fuel rod pitch (an input to S-RELAP5)
d = fuel rod diameter (cladding outer radius x 2)

Following fuel rod rupture, the Exxon Nuclear Company WREM II-based blockage model (Reference 44) is used. The model diverts flow from the hot assembly to neighboring assemblies in the blockage plane, and returns flow above the blockage region. The blockage is applied over [] with maximum blockage applied to the [] length and with [] The blockage region accounts for rupture at different axial elevations for fuel rods within the assembly. To make the blockage model and the Appendix K rupture node length requirement consistent, the region in the vicinity of the rupture is modeled as four axial regions, each [] in length since the Appendix K requirement is that inside oxidation must occur in a node which is 3 inches or less in length after cladding rupture. The rupture node is assumed to be the [] of the blockage region. Note that this is the same method currently approved for use with Zircaloy cladding (Reference 41).

For M5 cladding the average assembly blockage fractions (B_s and B_t) at temperature ramp rates of [] are obtained by linear interpolation of the assembly blockage values in Table 5.4 (Reference 1, the blockage function is plotted on Pages K-33 and K-34), which is plotted in Figure 5.3. Note that the approved table runs from []. It is anticipated that this range will span the range of temperatures at which rupture will occur. For completeness, however, the values at [] are programmed to be used for rupture temperatures below [], and the values at [] are programmed to be used for rupture temperatures above 1200°C. Note that the presented blockage fractions were derived for Mark-B 15x15 PWR fuel and were approved for use with Mark-B 15x15 and Mark-BW 17x17 PWR fuel types with M5 cladding in Reference 1. The cross-sectional dimensions and lattice

structure of the HTP 15x15 and 17x17 PWR fuel designs are very similar to those for Mark-B 15x15 and Mark-BW 17x17 PWR fuel designs, respectively. Therefore, the assembly blockage curves approved in Reference 1 are also applicable to HTP 15x15 and 17x17 PWR fuel. In terms of assembly blockage fraction, the values for the HTP 14x14 PWR fuel design differ by only a few percent from those for the Mark-B 15x15 fuel design. The difference is within the accuracy of the data and technique used to derive the blockage values as described in Reference 1. Therefore, the M5 blockage model approved for use with Mark-B 15x15 and Mark-BW 17x17 PWR fuel in Reference 1 will be used for HTP 14x14, HTP 15x15, and HTP 17x17 PWR fuel designs with M5 cladding.

The average assembly blockage fraction (B^f) is obtained from one of the following relationships:

$$B^f = \frac{1}{N} \sum_{j=1}^N B_j \quad (5.12)$$

For evaluation of flow area, the average assembly blockage fraction (B^f) is applied to the rupture node ($J = JS$) and the node above the rupture node ($J = JS+1$). The assembly average blockage fractions for the node below the rupture node ($J = JS - 1$) and the second node above the rupture node ($J = JS + 2$) are []. For all other nodes, the blockage fractions are [].

That is,

$$B_j = \begin{cases} B^f & \text{for } j = JS \text{ and } j = JS+1 \\ B^f & \text{for } j = JS-1 \text{ and } j = JS+2 \\ B_j & \text{for all other } j \end{cases} \quad (5.13)$$

The rupture node assembly average blockage fraction is used to adjust the unblocked flows in the blockage region and downstream of the blockage. These flows are used in the computation of heat transfer coefficients. Table 5.5 gives the flow as a fraction of the unblocked flow and distance from the center of the rupture node for assembly average blockage fractions of 20%

and 30%. The flow fractions (F_j^f) are assumed linear and are defined by the 20% and 30% blocked values in Table 5.5. Note that the application of the blockage fraction is the same as the model approved for use with Zircaloy cladding (Reference 41).

The elevation dependent mass fluxes ($W_{j,e}$) are computed by the following relationship:

5.14

The ratio of [] is then used to adjust the steam heat transfer coefficient for the hot rod.

**Table 5.1 Comparison of Young’s Modulus for
M5 and Zircaloy Cladding**

Table 5.2 M5 Cladding Rupture Strain

Table 5.3 M5 Cladding Pre-Rupture Strain

Table 5.4 M5 Cladding Assembly Blockage Fraction

Table 5.5 Unblocked Flow Fraction



Figure 5.1 M5 Slow and Fast Heating Ramp Rate Rupture Strain

Figure 5.2 M5 Slow and Fast Heating Ramp Rate Pre-Rupture Strain

**Figure 5.3 M5 Slow and Fast Heating Ramp Rate
Assembly Blockage**

6.0 PWR Mechanical Analysis Methodology

The description of the incorporation of M5 in the Group M PWR Mechanical Analysis Methodology that follows is organized in accordance with the Standard Review Plan 4.2 (Reference 45).

6.1 Fuel System Damage

6.1.1 Stress

The design basis for fuel component stresses per the approved methodology of Reference 3 specifies that the fuel system will not be damaged due to excessive stresses. Conservative limits are derived from the ASME Boiler Code (Code), Section III, Division 1, Article III-2000 (see Reference 46). The stress limits are based on the minimum specified 0.2% offset yield strength and the ultimate strength of the unirradiated cladding.

For application with M5, the approved unirradiated yield strengths of M5 are also used in the criteria. For the cladding, however, the hoop yield strength, derived from bi-axial tests, is used instead of the axial tensile strength. The limiting stresses are in the circumferential direction (the maximum shear stress is the circumferential minus the small radial stress) so use of the higher circumferential clad yield strength as compared to the usual axial tensile strength limit is acceptable. In addition for cladding, the allowed beginning of life (BOL) membrane stress in compression is extended to the hoop yield stress rather than two-thirds of this stress. These criteria are as approved in Reference 1.

The design tensile yield strength of M5 for structural materials (Reference 1) is given by:



6.1

The design hoop bi-axial yield strength for M5 cladding (Reference 1) is given by:



6.2

6.1.2 Strain (RODEX2-2A)

FRA-ANP's design criteria for Zircaloy fuel rod cladding strain (Reference 3) specifies that the total mean circumferential strain shall not exceed [

] (Reference 3, Section 3.2.5). This criterion is revised for applications with M5 clad per the approved Reference 1 to a limit of 1% for rod burnups to 62 GWd/MTU.

The methodology to evaluate the cladding strain uses the RODEX2-2A code (References 8 and 9) to simulate the most demanding fuel rod power histories with the most conservative combination of pellet and cladding properties in order to maximize end-of-life (EOL) cladding strain and to maximize cladding ramp strains. This methodology is unchanged.

As discussed in Section 4.0, the RODEX2-2A code is revised to incorporate the approved material properties applicable to M5 cladding. The M5 properties incorporated as described in Section 4.1 are:

- Clad Thermal Conductivity
- Oxide Thermal Conductivity
- Clad Coefficient of Thermal Expansion
- Clad Modulus of Elasticity
- Poisson's Ratio
- Clad Emissivity
- Clad Corrosion
- Clad Hydrogen Pickup

RODEX2-2A is also re-benchmarked for additional properties for which the existing M5 correlations are not directly compatible with the RODEX2-2A formulation of the irradiated fuel rod behavior. These characteristics are:

- Clad creep
- Axial elongation

Their benchmarking is described in Sections 4.2 and 4.3.

6.1.3 Strain Fatigue (RAMPEX)

The cladding fatigue evaluation is based on the cyclic stress amplitudes calculated for the specified number of duty cycles during the irradiation life using the O'Donnell and Langer (Reference 47) fatigue design curve. This criterion, approved in the existing methodology per Reference 3, was shown to be conservative for M5 per Reference 1 based on M5 cyclic strain fatigue tests.

The methodology to evaluate the stress cycles is based on the RODEX2 and RAMPEX codes. The RODEX2 code (revision of Reference 8) is a predecessor to the approved RODEX2-2A. It was benchmarked in conjunction with RAMPEX for determining pellet-clad interaction (PCI) stress. The RODEX2 code is used first to calculate the pseudo steady-state deformations of the pellet and cladding. The RAMPEX code uses the RODEX2-calculated deformations as the starting point for calculating stresses during power ramps. Changes in clad stress are evaluated to determine a fatigue usage factor, which is conservatively limited to [] (Reference 3) and to [] for M5 material per Reference 1. The higher limit [] is utilized via its approval for M5.

The same M5 clad properties as incorporated in RODEX2-2A are incorporated in RODEX2 to assure that the clad and pellet-starting condition for ramps is properly determined for M5 clad rods.

The RAMPEX code was similarly revised to incorporate the same M5 clad material properties described in Section 4.1 as applicable to power ramps. These are:

- Clad Thermal Conductivity
- Oxide Thermal Conductivity
- Clad Coefficient of Thermal Expansion
- Clad Modulus of Elasticity
- Poisson's Ratio
- Clad Emissivity

The clad creep correlation as benchmarked for RODEX2 per Sections 4.2 and 4.3 is also incorporated in RAMPEX. The clad corrosion, hydrogen pickup, and the irradiation component of axial elongation are not incorporated, as these are not necessary for evaluating ramp stresses.

For the stress-strain curve in RAMPEX, the cold worked stress relieved (CWSR) Zircaloy-4 property is retained for simplicity and for conservatism in the evaluation of the fatigue stresses. The stresses during ramps are evaluated against the fatigue usage criteria using the O'Donnell and Langer design curve, which is described in terms of stress amplitude. The use of the higher CWSR material yield strength, therefore, assures that plastic strain during the ramp is minimized resulting in the maximum calculated stresses. As a result, these stresses are conservatively determined and are on the same basis as used in fatigue design criterion of O'Donnell and Langer.

6.1.4 Fretting Wear

FRA-ANP's design basis for fretting corrosion and wear specifies that fuel rod failures due to fretting shall not occur (Reference 3, Section 3.3.3). Fretting wear depends chiefly on spacer grid and rod retention system design features and on the hydraulic environment in which the fuel rod operates.

Because significant amounts of fretting wear can eventually lead to fuel rod failure, spacer grid assemblies are designed to prevent such wear. In addition, FRA-ANP performs fretting tests to verify consistent fretting performance for new spacer designs. Examination of a large number of irradiated rods has substantiated the appropriateness of the fretting tests. Based on its similar composition, as well as the results of post-irradiation fuel rod inspections, FRA-ANP expects M5 cladding and grid spacers to exhibit the same fretting wear behavior as Zircaloy-4.

The NRC evaluation of fretting wear in the M5 topical report (Reference 1) concluded that a change in cladding material should not have a significant impact on fretting wear. The fretting criterion defined in the M5 topical report and in the FRA-ANP Group M generic criteria topical report (Reference 3) is essentially identical, both are consistent with SRP 4.2. The method of confirmation that fretting will not occur is similar between Reference 1 and Reference 3 in that both rely on a 1000-hour fretting test and in-reactor experience. Fretting tests have been performed for each of the assembly designs manufactured by FRA-ANP.

6.1.5 Oxidation, Hydriding, and Crud

The FRA-ANP Reference 3 approved design basis for corrosion of Zircaloy clad fuel rods specifies a [] This differs from the 100 micron criterion, as the limit applies to measurements made on a "peak local" rather than

running average basis, and because the data have been processed to develop a 95/95 statistical bound. The oxidation and hydriding for Zircaloy-4 are then calculated with the design equation for the most demanding power history in RODEX2-2A.

For M5 clad fuel rods, the approved M5 corrosion maximum best estimate equation (Reference 2) will be utilized. The M5 oxidation and hydriding equations are incorporated in RODEX2-2A as described in Section 4.0. The most demanding power history will thus be used in conjunction with the oxidation equation for the M5 clad and compared with the maximum 100 μm oxide limit approved for M5 application (Reference 1).

The M5 fuel rod oxide thickness measurements, corrosion equation, and the 100-micron criteria are on a consistent basis. M5 cladding is expected to meet this corrosion criterion by a wide margin, up to a burnup of 62 MWd/kgU.

6.1.6 Rod Bow

Differential expansion between fuel rods and guide tubes, as well as lateral thermal and flux gradients, can lead to lateral creep rod bow in the spans between spacer grids. This lateral creep bow changes rod-rod gaps in the span between spacer grids and may affect the peaking and local heat transfer. The FRA-ANP design basis for fuel rod bowing specifies that lateral displacement of the fuel rods shall be sufficiently small that it does not affect thermal margins (Reference 3, Section 3.3.5).

To evaluate the effect of rod bow on thermal margins, FRA-ANP uses a conservative rod bow projection, which is linear with burnup. Extensive post-irradiation inspections of Zircaloy-4 fuel assemblies have confirmed that rod bow has not reduced spacing between adjacent rods by more than 50%. The potential effect of greater bow on thermal margins is negligible because of the lower power achieved at high exposure.

The use of M5 material in rods and guide tubes is expected to have little, or possibly, a beneficial effect on the occurrence of rod bow. Rod bow is, in part, due to the forces on the rod resulting from differential expansion between the rod and guide tubes. The overall lower growth of the M5 material should reduce differential growth and the potential for bow induced by axial forces.

6.1.7 Axial Growth

The FRA-ANP generic methodology (Reference 3) uses bounding empirical models to compute the irradiation growth of the clad and fuel assemblies. The bounding models are established by a 95/95 statistical evaluation of the growth measurements. The resulting dimensional changes are then compared with the available clearances, including the component and core tolerance accumulations. The 95/95 bounding models may be re-correlated as additional data becomes available. These re-correlations need not be submitted if the new correlation is within one standard deviation of the referenced correlation.

6.1.7.1 Fuel Rod Growth

The clearance between the upper and lower tie plate shall be designed to accommodate the maximum differential fuel rod and fuel assembly growth to the design burnup. The upper bound fuel rod growth is used in conjunction with the lower bound assembly growth and the manufacturing tolerances that would result in the minimum fabricated clearance. An M5 fuel rod elongation correlation is available from the approved Reference 1. It is updated with additional irradiated fuel measurements and is shown in Figure 6.1. The re-correlated nominal projection and 95/95 upper and lower bounds are described by the following equations:

Figure 6.1

6.3

where

$$\begin{aligned} \frac{\Delta L}{L_o} &= \text{Elongation (\%)} \\ \phi_1 &= \text{Fluence (n/cm}^2\text{), E>1 MeV} \end{aligned}$$

These equations are valid up to a fluence of 14×10^{21} n/cm². The additional data, primarily from U.S. reactors, broadens the statistical distribution towards lower rod growth. The maximum growth is similar to that previously submitted. These bounds are $\pm 42.6\%$ of the nominal.

6.1.7.2 Fuel Assembly Growth

The fuel assembly growth shall not exceed the minimum space between the upper and lower core plates in the reactor in the cold condition. The cold condition is limiting since the thermal expansion coefficient of the stainless steel core barrel is greater than the coefficient of expansion of Zircaloy-4 or M5 guide tubes.

Although additional M5 assembly growth data have been obtained since the approval of Reference 1, there is still not sufficient data for a statistical bound. When sufficient assembly growth data are obtained, 95/95 maximum and minimum assembly growth curves may be derived. These equations will be based on the form of the rod growth equation, and may be prepared on a generic or design specific basis.

Until sufficient assembly growth data are obtained for statistical projections, the M5 fuel assembly growth and tolerance limits will be developed from [

]

The M5 assembly growth data and bounds are plotted in Figure 6.2. As expected, the data show variability between different assembly configurations. Such variation has been seen for Zircaloy-4 structure FRA-ANP assemblies where different growth correlations have been developed for different assembly types. The M5 assembly design bounds are conservative for the following reasons:

[

1

6.1.8 Rod Internal Pressure

To prevent unstable thermal behavior and to maintain the integrity of the cladding, FRA-ANP limits the maximum internal rod pressure to system pressure plus [. . .] psi (Reference 3, Section 3.3.7). When the fuel rod internal pressure exceeds system pressure, the pellet-cladding gap has to remain closed if it is already closed, or it should not tend to open for steady or increasing power conditions. Outward circumferential creep, that may cause an increase in pellet-to-cladding gap, must be prevented since it would lead to higher fuel temperature and higher fission gas release. The maximum internal pressure is also limited to protect embrittlement of the cladding caused by hydride reorientation during cool down and depressurization conditions.

FRA-ANP calculates the rod internal gas pressure with the RODEX2-2A code. As discussed in Section 4.0, the RODEX2-2A code is revised to incorporate the approved material properties applicable to M5 cladding. The M5 properties incorporated as described in Section 4.1 are:

- Clad Thermal Conductivity
- Oxide Thermal Conductivity
- Clad Coefficient of Thermal Expansion
- Clad Modulus of Elasticity
- Poisson's Ratio
- Clad Emissivity
- Clad Corrosion
- Clad Hydrogen Pickup

RODEX2-2A is also re-benchmarked for additional properties for which the existing M5 correlations are not directly compatible with the RODEX2 formulation of the irradiated fuel rod behavior. These characteristics are:

- Clad creep
- Axial elongation

Their benchmarking is described in Sections 4.2 and 4.3.

The existing methods for evaluating the margin to the fuel rod pressure limit with the RODEX2-2A code will therefore be retained.

M5 cladding has a lower corrosion rate than Zircaloy-4 clad and a lower hydrogen pickup fraction. These results in lower hydrogen concentrations in M5 cladding than in Zircaloy-4 clad for the same reactor duty. The pressure stresses in M5 clad will be the same as those in Zircaloy-4 cladding for the same operational conditions. Because the same design pressure criterion [] is chosen for the M5 clad fuel rods, the limiting hydride reorientation behavior will be bounded by that for Zircaloy-4. The design criterion pressure limit used for Zircaloy-4 is therefore conservative and applicable for M5 cladding.

6.1.9 Assembly Liftoff

The FRA-ANP design criterion for assembly liftoff specifies that the assembly shall not levitate from hydraulic loads (Reference 3, Section 3.3.8). Therefore, for normal operation and anticipated operational occurrences, the submerged fuel assembly weight and holddown force must be greater than the upward hydraulic loads.

M5 cladding and structural material has a small effect due to the change in material density affecting the weight, and the change in coefficient of thermal expansion and assembly growth affecting the bundle length and thus the holddown spring force. The density and thermal expansion properties are approved in Reference 1. The length projections are revised with additional data in Section 6.1.7.2. These changes will be implemented in the liftoff calculations.

6.1.10 Fuel Assembly Handling

The assembly design must withstand all normal axial loads from shipping and fuel handling operations without permanent deformation. FRA-ANP uses either a stress analysis or testing to

demonstrate compliance. The analysis or test uses an axial load of 2.5 times the static fuel assembly weight. At this load, the fuel assembly structural components must not show any yielding.

For these evaluations, the M5 density will be used to determine M5 component weights, and the M5 tensile strength will be used to determine strength margins.

6.1.11 Control Rod Reactivity

FRA-ANP's design basis for the fuel assembly specifies that the Technical Specification shutdown margin will be maintained (Reference 3, Section 5.2). Specifically, the assemblies and core must be designed to remain subcritical with the highest reactivity worth control rod fully withdrawn and the remaining control rods fully inserted. Shutdown margin is calculated and demonstrated at the beginning of the cycle (as a minimum) for each reactor. FRA-ANP uses standard approved design methods to ensure that adequate limits are placed on control rod worth.

The change in alloy content from approximately 1.4% tin in the Zircaloy-4 to 1.0% Niobium in the M5 will tend to slightly increase the neutron absorption cross-section of the M5 compared to Zircaloy-4. This change in cross section has a negligible impact on control rod worth.

6.2 **Fuel Rod Failure**

6.2.1 Hydriding (Internal)

FRA-ANP reduces the potential for hydrogen absorption on the inside of the cladding by eliminating potential sources of moisture during fuel rod fabrication, including the careful control of fuel pellet moisture content. By controlling the moisture content of the fuel pellets, the fabrication limit for total hydrogen inside the fuel rod is maintained at a minimal level (Reference 3, Section 3.2.1).

The absorption of hydrogen by fuel rod cladding can result in cladding failure due to reduced ductility and the formation of hydride platelets. To verify that acceptably low levels of hydrogen are being maintained, a statistical sample of fabricated pellets is selected for analysis, and the hydrogen content is measured and compared to the established limit. FRA-ANP has experienced no significant level of fuel failures due to internal hydriding, confirming that the testing and sampling processes permit adequate control of moisture within the fuel rods.

FRA-ANP will continue its current practice for controlling internal hydrogen concentration; internal hydriding experience with M5 cladding is expected to be the same as for Zircaloy-4 cladding.

6.2.2 Cladding Collapse

The FRA-ANP cladding creep collapse criterion is designed to prevent the formation of significant axial gaps in the fuel pellet column due to pellet densification (Reference 3, Section 3.2.2). The opening of axial gaps in the pellet column creates the potential for cladding to collapse (flatten) into the gap, where the large local strains resulting from cladding collapse could be sufficient to cause clad failure. Thus, the cladding creep collapse criterion is established to preclude cladding collapse during the design lives of fuel rods and burnable absorber rods.

The methodology used to demonstrate compliance with the cladding creep collapse criterion determines whether pellet hang-up can occur during the [

]. The collapse criterion specifies that cladding uniform creepdown (calculated with RODEX2-2A), combined with an ovality increase (calculated with COLAPX), shall not cause the pellets to become locked up inside the cladding. If the pellets are free to move axially, the pellet column can consolidate due to densification and, under the force of the fuel rod plenum spring, prevent the formation of axial gaps. FRA-ANP's collapse criterion requires that the cladding inner diameter decrease due to the combined effects of cladding creepdown and ovality increase [] be less than the initial minimum diametrical gap. This approach conservatively neglects pellet densification. Both uniform creepdown and ovality increase, which are combined together to evaluate the degree of diametrical gap closure, are controlled by the creep strain rate of the cladding.

As described in Section 4.0, the M5 properties are incorporated in the RODEX2-2A code that calculates radial creepdown, and also provides pressure and temperature information to the COLAPX code which then predicts the development of creep ovality. The RODEX2-2A benchmarking was used to determine the M5 creep coefficients to use with the existing COLAPX creep model. The existing COLAPX elastic modulus was not changed from that of Zircaloy as in the applicable temperature range, the slight modulus increase for M5 (about 1%) will have a negligible effect on the calculated creep ovality.

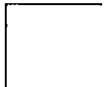
The COLAPX code does not model the entire fuel rod, and thus is not suitable for direct M5 creep benchmarking. A RODEX2 code version, which contains the COLAPX creep model and has the whole fuel rod modeling capability, was used in the COLAPX M5 creep model benchmarking. The creep model is:

Low temperature region model:



6.4

and high temperature region model:



6.5

where:

FLUX = FLUX E.GT.1 Mev [n/cm² sec]
T = temperature (°F)
 σ_c = generalized stress (psi)

The best-fit coefficients for COLAPX creep model were determined as follows:



Figures 6.3 and 6.4 display the benchmarking results. Both figures show that with the best-fit creep coefficients, the COLAPX creep model properly predicts the M5 creep data.

The approved procedure using RODEX2-2A and COLAPX is therefore used with M5 properties incorporated in RODEX2-2A and with the creep projections for RODEX2-2A and COLAPX benchmarked to M5 rod data.

6.2.3 Overheating of Cladding

The design basis to preclude fuel rod cladding overheating specifies that there must be at least 95% probability at a 95% confidence level that any fuel rod in the core does not experience departure from nucleate boiling (DNB) during steady-state operation and anticipated operational occurrences (Reference 3, Section 3.2.3).

6.2.3.1 Effect of M5 Cladding on DNB Phenomena

Overheating of the cladding occurs when there is a sharp reduction in the surface heat transfer coefficient caused by the formation of an insulating vapor layer on the cladding surface. This phenomenon is commonly called departure from nucleate boiling, or DNB. The parameters that dominate the heat flux at which DNB occurs include: 1) the mechanical design of the fuel assembly, in particular, the spacer grid which is designed to strip the vapor layer from the cladding surface; and 2) the fluid conditions, such as mass flux, pressure, and quality. The cladding material and its thermal conductivity and heat capacity have no significant effect on the surface heat transfer coefficient and surface heat flux at which DNB occurs. When a vapor layer exists on the cladding surface, the fuel rod is not conduction limited, and the rod heat flux is dominated by the surface heat transfer coefficient. Therefore, there is no significant effect of either M5 cladding or Zircaloy-4 cladding on DNB phenomena.

6.2.3.2 Effect of M5 Cladding on DNBR Criterion

Fuel cladding integrity is maintained by ensuring that the minimum departure from nucleate boiling ratio (DNBR) remains above the 95/95 DNB correlation limit for a given fuel design. The 95/95 DNB correlation limit is derived from DNB test data. As indicated above, neither M5 nor Zircaloy-4 cladding has a significant effect on DNB phenomena. Thus, Inconel clad heater rods in DNB tests typically simulate fuel assemblies. Therefore, use of M5 cladding will have no effect on the DNB data or the DNBR criterion (95/95 DNB correlation limit).

6.2.4 Overheating of Fuel Pellets

The design criterion for overheating of fuel pellets specifies that the centerline temperature of the fuel pellets must remain below the pellet melting temperature during normal operation and anticipated operational occurrences (Reference 3, Section 3.2.4).

The centerline-melting criterion was established to assure that axial or radial relocation of molten fuel would neither allow molten fuel to come into contact with the cladding nor produce local hot spots. For normal operation and anticipated operational occurrences, centerline melting is not permitted. In calculations of radiological dose for the case of postulated accidents, all rods that experience centerline melting are assumed to fail. This assumption that centerline-melting results in fuel failure is conservative.

The margin to centerline melting is calculated with the RODEX2-2A code in which predictions of fuel temperature are dependent on linear heat rate, the fuel properties, the state of the pellet-clad gap, and the thermal conductivity of the clad. As described in Section 4.0, the properties for M5 cladding have been incorporated into the RODEX2-2A code. Therefore, the existing methods for evaluating the margin to fuel melting with the RODEX2-2A code will be using the applicable M5 properties.

6.2.5 Pellet-Cladding Interaction

The SRP does not contain explicit criteria to address PCI; however, it does present three related criteria:

1. The uniform strain of the cladding should not exceed 1%. In this context, uniform strain (elastic and inelastic) is defined as transient-induced deformation with gage lengths corresponding to cladding dimensions.
2. Fuel melting should be avoided. The large volume increase associated with melting may cause a pellet with a molten center to exert a stress on the cladding.
3. Clad fatigue usage shall be limited. Cyclic loading associated with relatively large changes in power can cause cumulative damage, which may eventually lead to fatigue failure.

These criteria are unaffected by the change from Zircaloy-4 to M5. Incorporation of M5 properties in the methodology to address these criteria is described in Sections 6.1.2, 6.1.3, and 6.2.4.

6.2.6 Cladding Rupture

The approved M5 cladding rupture model (Reference 1) is incorporated in the S-RELAP5 methodology (Reference 41) as described in Section 5.1.14.

6.2.7 Mechanical Fracturing

Accident evaluation of the fuel assembly is performed in accordance with previously approved methodology (References 13 and 14). Determination of assembly loads is typically performed with a dynamic analysis. For this analysis, the change in properties from Zircaloy-4 to M5 must be considered. The properties, which affect dynamic response, are the material density and modulus of elasticity.

For conversion from an assembly with Zircaloy-4 to M5 structure, the combined effect of modulus change and material density change for all the assembly components on the fuel assembly frequency will be small. Considering that about 20% of the assembly weight is Zircaloy-4 or M5, and the M5 density is 99% of the Zircaloy-4 density, the change in mass from an all Zircaloy-4 to all M5 clad and structure would be -0.2%. At operating temperature of about 577 K (579°F), the change in assembly stiffness due to the modulus change will be +1.8%, assuming that all the assembly stiffness is due to Zircaloy or M5 structure. This would result in an assembly frequency change of about +1% ($\sqrt{\frac{1.018}{0.998}} - 1$). Existing dynamic analysis loads for such a material conversion will therefore be retained; however, as described below, the strength characteristics will be reevaluated. For new dynamic evaluations, the approved M5 properties (Sections 4.1.8 and 5.1.6) for the applicable M5 components will be used for both determining dynamic response and strength margins.

FRA-ANP limits the combined stresses from postulated accidents to the stress limits given in ASME Code Section III, Appendix F for faulted conditions (Reference 3, Section 3.2.7).

Cladding and guide tube integrity are determined to be maintained if the applied stress is less than 90% of the irradiated yield stress at the appropriate temperature. The BOL yield strength is used as a conservative lower bound on the irradiated yield strength.

The approved (Reference 1) tensile yield strength of the M5 cladding and guide tubes (Section 6.1.1) will be used in this evaluation. M5 spacer grids, if used, will be evaluated by strength testing of the specific M5 grid design as described in the methodology (References 13 and 14).

6.3 ***M5 Sample Fuel Rod Analysis***

6.3.1 Summary of Sample M5 Rod Analysis

A design description and the results of fuel rod mechanical analyses are provided. The analysis includes the fuel rod thermal-mechanical calculations for normal operation and anticipated transient conditions.

The analyses were performed using NRC-approved mechanical design analysis methodology as revised per this report for the incorporation of M5 clad material properties.

The analyses demonstrate that the mechanical design criteria for the fuel rod are satisfied for the sample peak fuel rod average exposure of 70,000 MWd/MTU.

6.3.2 Assembly Design

The mechanical design for the sample rod analysis is a CE-type 14x14 assembly configuration with M5 clad rods, Zircaloy-4 guide tubes, a FUELGUARD™* lower tie plate (LTP), and Zircaloy-4 HTP spacers.

The fuel rod design has 0.440-inch outer diameter [] M5 clad containing enriched uranium dioxide pellets and an Alloy X-750 plenum spring. The fuel pellets are sintered to an initial nominal density of [] of theoretical density. Table 6.1 shows the fuel design parameters.

6.3.3 Rod Mechanical Evaluation

Table 6.2 provides a summary of the reactor information that was used for the mechanical design evaluation. The fuel was analyzed using typical 14x14 design operating conditions to a rod exposure of 70 GWD/tU.

Power history inputs are used to evaluate cladding and fuel pellet thermal-mechanical criteria. Fuel rod power histories for the limiting cases are shown in Figures 6.5 and 6.6. The two figures are plots of rod average LHGR and peak rod nodal LHGR versus exposure. Table 6.3 lists the design duty cycles that were used as inputs for the cyclic fatigue analyses.

* FUELGUARD is a trademark of Framatome ANP, Inc.

The fuel rod design was evaluated using approved mechanical design methods as revised by this report. Table 6.4 summarizes the results of the design evaluations. Table 6.5 details the results of the clad stress calculation. Plots of the clad corrosion and fuel rod gas pressure results are shown in Figures 6.7 and 6.8 for the limiting cases. Figure 6.7 shows the predicted maximum oxide thickness versus exposure. Figure 6.8 provides the maximum rod internal pressure versus exposure.

Table 6.1 Fuel Assembly and Rod Description



Table 6.2 Reactor Operating Conditions for Mechanical Evaluation

Parameter	Value
Core Thermal Power, MWt	2700
System Pressure, psia	2250
Number of Assemblies	217
Nominal Total Core Flow Rate, Mlbm/hr	149.4
Core Inlet Temperature, °F	548.0
Core Outlet Temperature, °F	597.0
Maximum Overpower, %	117
Fraction of Heat from Fuel Rods	0.975
Core Average LHGR, kW/ft	6.20
Maximum LHGR, kW/ft	14.3
Maximum Rod Peaking Factor, F_R^T	1.65
Peak Rod Burnup, GWd/MTU	70.0

Table 6.3 Design Duty Cycles for Cyclic Fatigue Evaluation

A.	Refueling - 1 per Reactor cycle 0% - 50% @ 15%/hr Reactor Power above 50% - maximum power escalation rate, 3%/hr
B.	Hot Standby - 10 per year 0% - 100% @ 5%/min
C.	Load Follow - 250 per year 15% - 100% @ 5%/min
D.	Step Load Change - 50 per year From 15% and 90% to 100%, 10% step change
E.	Cold Shutdown - 11 per year 0% - 100% @ 50%/min

Table 6.4 Mechanical Fuel Design Evaluation Results

* Section numbering per generic design criteria Reference 3.





Table 6.5 Clad Stress Intensity Results

-
- * Primary membrane EOL hot criteria equals $\frac{2}{3}$ yield for clad in tensile stress condition, for other primary membrane evaluations criteria is 1.0 yield for compressive stress condition.




Figure 6.1 M5 Fuel Rod Growth



Figure 6.2 M5 Assembly Growth



**Figure 6.3 Comparison of COLAPX M5 Cladding Creep Model
Calculated Radial Creep to Measured Creep**



**Figure 6.4 COLAPX M5 Creep Model - Calculated Radial Creep and
Measured vs. Local Burnup**



**Figure 6.5 Fuel Rod Power History Inputs For Limiting Cases - Rod
Average LHGR**



**Figure 6.6 Fuel Rod Power History Inputs For Limiting Cases - Peak
Rod Nodal LHGR**



Figure 6.7 Predicted Maximum Fuel Rod Oxidation

Figure 6.8 Calculated Rod Internal Pressure versus Exposure

7.0 S-RELAP5 Based Appendix K PWR SBLOCA Methodology

The addition of approved M5 cladding properties and models to the two computer codes used in the approved S-RELAP5 based Appendix K PWR SBLOCA methodology (RODEX2-2A and S-RELAP5) (Reference 4) is straightforward and was described in Sections 4.0 and 5.0. As a result, the methodology for performing SBLOCA calculations that was approved in Reference 4 is unchanged except to add the properties specific to M5 cladding. However, some M5 properties that were required for SBLOCA analyses were either not available in the approved documents, required a range of applicability that extended outside the approved range, or required a new correlation for model-specific usage. These properties include creep, growth, thermal expansion, emissivity, elastic modulus, and rod rupture flow blockage. Where applicable, the modifications to the approved M5 properties have been discussed and justified in Sections 4.0 and 5.0.

It is expected that changing cladding type to a material similar to Zircaloy, such as M5, will have an insignificant impact on important criteria for SBLOCA analyses. The results from the sample problem discussed in Section 7.4 confirm this expectation. The analysis shows that little variation in calculated peak cladding temperature (PCT) or oxidation occurs when M5 cladding is substituted for Zircaloy cladding in an SBLOCA calculation.

7.1 Methodology Summary

The approved methodology for evaluation of SBLOCA transient response for both CE and Westinghouse design PWRs is described in EMF-2328(P)(A) (Reference 4). The use of M5 cladding affects the fuel rod model used in this methodology. The purpose of the SBLOCA analysis is to demonstrate that the criteria stated in 10CFR 50.46(b) are met under the conditions of a SBLOCA. These criteria are as follows:

1. The calculated maximum fuel element cladding temperature shall not exceed 2200°F.
2. The calculated local fuel rod cladding oxidation shall nowhere exceed 17% of the total cladding thickness before oxidation.
3. The calculated total amount of fuel element cladding, which reacts chemically with water or steam, shall not exceed 1% of the Zircaloy within the heated length of the core.
4. The cladding temperature transient shall be terminated at a time when the core geometry is still amenable to cooling.
5. The core temperature shall be reduced and decay heat shall be removed for an extended period as required by the long-lived radioactivity remaining in the core.

S-RELAP5 is the principal computer code used for analysis of the SBLOCA event. Before the analysis can be performed, S-RELAP5 requires initial fuel rod conditions. The rod conditions are determined by RODEX2-2A where the fuel burnup is calculated to the desired burnup level, usually end of cycle conditions. The RODEX2-2A results at the desired burnup are transferred to S-RELAP5. A steady-state calculation using S-RELAP5 is made that initializes the system model to plant operating conditions. After assuring the steady-state calculation is representative of the plant operating conditions, the SBLOCA transient is performed. In addition to calculating the overall system thermal-hydraulic response, S-RELAP5 also concurrently calculates the hot rod temperature transient using the hot rod input including RODEX2-2A fuel models and the NUREG-0630 swelling and rupture models for analyses with Zircaloy cladding. The approved swelling and rupture models for M5 (Reference 1) have now been incorporated into S-RELAP5 for analyses with M5 cladding.

After calculations and analyses have been made to determine the limiting single failure, a break spectrum is analyzed by making several calculations with varying break sizes. From this calculation set, the results are examined to determine the break size having the greatest PCT or maximum oxidation present. The calculation having the greatest PCT or maximum amount of cladding oxidized in the break spectrum is the limiting SBLOCA break yielding the reportable PCT, and becomes the analysis of record. The results of this analysis are also compared to the criteria in 10CFR 50.46(b) for reporting purposes.

7.2 Summary of Clad Related Models in the SBLOCA Methodology

7.2.1 RODEX2-2A

The RODEX2-2A code is used to perform the fuel burnup calculation before initiating the S-RELAP5 calculation. As described in Section 4.0, the cladding related models implemented in RODEX2-2A for M5 cladding are:

- Cladding Creep
- Cladding free growth (and Axial Elongation)
- Cladding Thermal Conductivity
- Oxide Thermal Conductivity
- Cladding Coefficient of Thermal Expansion
- Cladding Modulus of Elasticity
- Cladding Poisson's Ratio

- Cladding Emissivity
- Cladding Corrosion

Cladding surface roughness is another cladding related parameter that is specified in user input.

7.2.2 S-RELAP5

The S-RELAP5 code is used to perform the transient SBLOCA calculation. It performs the system thermal-hydraulic calculation as well as the hot rod heat-up, rupture, and deformation calculations. As described in Section 5.0, the cladding related models implemented in S-RELAP5 for M5 cladding are:

- Cladding Thermal Conductivity
- Oxide Thermal Conductivity
- Cladding Specific Heat
- Cladding Density
- Cladding Coefficient of Thermal Expansion
- Cladding Modulus of Elasticity
- Cladding Poisson's Ratio
- Cladding Emissivity
- High Temperature Cladding/Steam Reaction Kinetics
- Cladding Swelling and Rupture/Blockage

Cladding surface roughness is another cladding related parameter that is specified in user input.

7.3 ***M5 Properties and Correlations Implemented in SBLOCA Models***

7.3.1 Cladding Creep Correlation

M5 cladding creep for SBLOCA calculations is implemented in the rod burnup calculation as discussed in Section 4.1.1 in the RODEX2-2A code. Note that cladding creep is a burnup dependent parameter. The duration of an S-RELAP5 SBLOCA calculation is sufficiently short to hold burnup dependent parameters constant. Therefore, cladding creep is not calculated in the S-RELAP5 code.

7.3.2 Cladding Free Growth

M5 cladding free growth for SBLOCA calculations is implemented in the rod burnup calculation as discussed in Sections 4.1.2 and 4.3 in the RODEX2-2A code. Note that cladding free growth

is a burnup dependent parameter. The duration of an S-RELAP5 SBLOCA calculation is sufficiently short to hold burnup dependent parameters constant. Therefore, cladding free growth is not calculated in the S-RELAP5 code.

7.3.3 Cladding Thermal Conductivity

M5 cladding thermal conductivity for SBLOCA calculations is implemented as discussed in Section 4.1.3 and 5.1.3 in the RODEX2-2A and S-RELAP5 codes, respectively.

7.3.4 Cladding Oxide Thermal Conductivity

M5 cladding oxide thermal conductivity for SBLOCA calculations is implemented as discussed in Section 4.1.4 and 5.1.4 in the RODEX2-2A and S-RELAP5 codes, respectively.

7.3.5 Cladding Specific Heat

M5 cladding specific heat for SBLOCA calculations is implemented in the transient calculation as discussed in Section 5.1.5 in the S-RELAP5 code. Note that cladding heat capacity is not used in the RODEX2-2A code. RODEX2-2A calculations assume quasi-steady thermal conditions for each burnup interval so specific heat is not required.

7.3.6 Cladding Density

M5 cladding density for SBLOCA calculations is implemented in the transient calculation as discussed in Section 5.1.6 in the S-RELAP5 code. Note that cladding density is not used in the RODEX2-2A code. Density would be multiplied by the specific heat to provide a volumetric heat capacity. However, RODEX2-2A calculations assume quasi-steady thermal conditions for each burnup interval so heat capacity and density are not required.

7.3.7 Cladding Thermal Expansion

M5 cladding thermal expansion for SBLOCA calculations is implemented as discussed in Section 4.1.7 and 5.1.7 in the RODEX2-2A and S-RELAP5 codes, respectively.

7.3.8 Cladding Modulus of Elasticity

M5 cladding Young's modulus for SBLOCA calculations is implemented as discussed in Section 4.1.8 and 5.1.8 in the RODEX2-2A and S-RELAP5 codes, respectively.

7.3.9 Poisson's Ratio

M5 cladding Poisson's Ratio for SBLOCA calculations is implemented as discussed in Section 4.1.9 and 5.1.9 in the RODEX2-2A and S-RELAP5 codes, respectively.

7.3.10 Cladding Emissivity

M5 cladding emissivity for SBLOCA calculations is implemented as discussed in Sections 4.1.10 and 5.1.10 in the RODEX2-2A and S-RELAP5 codes, respectively.

7.3.11 Cladding Corrosion

M5 cladding corrosion for SBLOCA calculations is implemented in the burnup calculation as discussed in Section 4.1.11 in the RODEX2-2A code. Low temperature cladding corrosion is not calculated in S-RELAP5. The SBLOCA transient calculation performed by S-RELAP5 occurs over a short time period compared to the burnup calculation in RODEX2-2A and produces high cladding temperatures. When high temperatures occur, corrosion is accelerated and the low temperature corrosion models are no longer valid. At the high cladding temperatures predicted in the S-RELAP5 calculation, a special high temperature M5/steam reaction kinetics model is needed. Section 5.1.13 describes the high temperature M5/steam reaction kinetics model used in S-RELAP5.

7.3.12 Cladding Hydrogen Pickup

M5 cladding hydrogen pickup for SBLOCA calculations is implemented in the burnup calculation as discussed in Section 4.1.12 in the RODEX2-2A code. Cladding hydrogen pickup is not calculated in S-RELAP5. The cladding hydrogen pickup model described in Section 4.1.12 is associated with low temperature cladding corrosion. The SBLOCA transient calculation performed by S-RELAP5 produces high cladding temperatures where corrosion is accelerated and the low temperature corrosion models are no longer valid. A special high temperature M5/steam reaction kinetics model is then required as described in Section 5.1.13. Since the criteria for SBLOCA do not set limits on hydrogen pickup but only on cladding oxidation, the high temperature M5/steam reaction kinetics model only considers oxidation and not hydrogen pickup.

7.3.13 High Temperature M5/Steam Reaction Kinetics

Metal-water reaction kinetics for SBLOCA calculations is implemented in the transient calculation as discussed in Section 5.1.13 in the S-RELAP5 code. The RODEX2-2A calculations are performed at normal reactor operating conditions. The temperature of the cladding during normal operating conditions is not high enough for significant metal-water reaction to take place. Therefore, only low-temperature cladding corrosion models are used to determine cladding oxidation in the RODEX2-2A code.

7.3.14 Cladding Surface Roughness

Surface roughness is an input parameter that is more closely associated with the cladding manufacturing process than the cladding material type. Currently, manufactured surface roughness is input to the RODEX2-2A code for cladding internal surface roughness. This practice will continue with M5 cladding. It is not anticipated that M5 rod external surface roughness will differ substantially from Zircaloy cladding. Therefore, the same external surface roughness for the thermal-hydraulic calculation performed by S-RELAP5 will be used for M5 as is currently used for Zircaloy cladding (5.0×10^{-6} ft for typical drawn tubing, Reference 48, Page A-23).

7.3.15 Cladding Swelling and Rupture/Blockage

M5 cladding swelling and rupture model for SBLOCA calculations is implemented during the transient calculation in the S-RELAP5 code as discussed in Section 5.1.14. The RODEX2-2A code is used to calculate burnup dependent fuel behavior at normal reactor operating conditions. Under these conditions, swelling and rupture/blockage will not occur and, therefore, no swelling and rupture/blockage model is implemented in the RODEX2-2A code.

7.4 ***SBLOCA Sample Problem with M5 Cladding***

To evaluate PCT and oxidation sensitivity to M5 properties, a sample SBLOCA calculation was performed with both Zircaloy and M5 cladding specified. The sample problem is a 15x15 Westinghouse 3-loop PWR and is identical to the sample problem presented in the 1999 approved SBLOCA methodology (Reference 4). The scope of this analysis was to compare PCT and oxidation predictions between the models with Zircaloy and M5 cladding and to identify the major phenomenological contributors for any significant differences observed. It is not expected that the introduction of M5 cladding will produce PCT and core wide or maximum

oxidation for M5 rods that is significantly different from Zircaloy rods. These expectations are confirmed by the analysis.

The 3-loop SBLOCA sample problem presented in Reference 4 was rerun with two geometrically identical rod types: one with Zircaloy cladding and one with M5 cladding. The limiting values for the key acceptance criteria were then compared to identify any differences in SBLOCA behavior between the use of M5 and Zircaloy cladding. A 1½-inch, 2-inch, and 2½-inch SBLOCA calculation was performed. The analytical results show that the limiting PCT and oxidation break size is the same for both materials []. The M5 limiting PCT was calculated to be [] (vs. [] for the Zircaloy case) and the M5 limiting oxidation was calculated to be [] (vs. [] for the Zircaloy case). M5 core wide oxidation was calculated to be [] (vs [] for the Zircaloy case). Figure 7.1 shows excellent PCT agreement between the M5 and Zircaloy hot rods over the course of the transient.

Examination of the results from the SBLOCA calculations show that the steady-state cladding temperatures at the burn-up of interest [] are nearly identical between the two hot rod models; however, fuel centerline temperature for the M5 hot rod at the peak power location is [] than the Zircaloy case*. This variation is attributed to differences in cladding creep and tangential thermal expansion, which influence the fuel-clad gap width. The gap width effects fuel temperature and pellet-clad interactions throughout the burnup calculation in RODEX2-2A. Differences in fuel temperature and pellet-clad interactions can alter pellet material properties in the burnup calculation and, therefore, can affect initial stored energy. []

Initial stored energy, however, is not a parameter of primary importance for a SBLOCA transient calculation because core uncovering does not occur until well after reactor scram. Therefore, the difference in initial stored energy is not expected to greatly alter SBLOCA transient results.

Since rod rupture did not occur for the limiting SBLOCA case, an additional rupture case was created and run. The additional case is identical to the limiting [] break case except that the power has been increased by an additional [] power. The increased power causes an increased heat up which results in hot rod rupture. Figure 7.2 shows excellent PCT

* Centerline temperatures will be dependent on both material properties and local power factors. Actual rod-averaged changes in centerline temperature will be much smaller.

agreement between the M5 and Zircaloy hot rods over the course of the transient for this case. The M5 limiting PCT was calculated to be [] (vs. [] for the Zircaloy case) and the M5 limiting oxidation was calculated to be [] (vs. [] for the Zircaloy case). M5 core wide oxidation was calculated to be [] (vs. [] for the Zircaloy case). [

] Overall, however, the transient response between the Zircaloy and M5 cases is very similar and no substantially different phenomena can be identified.

**Figure 7.1 M5 PCT and Zircaloy PCT for the
Limiting PCT Calculation (2-inch Break)**

**Figure 7.2 M5 PCT and Zircaloy PCT for the
High Power 2-Inch Break**

8.0 Non-LOCA Methodology

The FRA-ANP non-LOCA methodology is composed of three approved methods: SRP Chapter 15 Non-LOCA Transient Methodology for Pressurized Water Reactors [EMF-2310(P)(A)], Statistical Setpoint/Transient Methodology for Westinghouse Type Reactors [EMF-91-081(P)(A)], and Statistical Setpoint/Transient Methodology for Combustion Engineering Type Reactors [EMF-1961(P)(A)] (References 5-7). A discussion is presented below about the issues related to cladding type that are important to each methodology. The implementation of M5 models applicable to the non-LOCA methodologies in the affected computer codes (RODEX2-2A and S-RELAP5) is then described. The description is followed by a sample problem for statistical setpoint/transient methodologies with M5 cladding.

8.1 Methodology Summary

8.1.1 SRP Chapter 15 Non-LOCA Transient Methodology

The approved methodology for evaluation of SRP Chapter 15 non-LOCA transients for both CE and Westinghouse design PWR's is described in EMF-2310(P)(A). The use of M5 cladding affects the fuel rod model used in this methodology. EMF-2310(P)(A) explicitly addresses the fuel rod model that is to be applied using S-RELAP5. Two options are available for the fuel rod model. The first option is the use of a heat structure based average fuel rod model that may include a hot spot model. The second option is to use the RODEX2 model that is internal to S-RELAP5. The XCOBRA-IIIC code [XN-NF-75-21(P)(A)] (Reference 20) is also used in the approved SRP Chapter 15 non-LOCA transient methodology but does not perform material property or deformation calculations for the clad or fuel.

The approved methodology, EMF-2310(P)(A), does not require revision to support M5 cladding.

[

]

The methodology prescribes the conditions under which the [] must be repeated due to changes in fuel design. The specific changes that cause reevaluation are (Reference 5, Page 3-3):

- Free volume to fuel ratio
- Cladding type (creepdown behavior)
- Porosity
- Change in certain RODEX2 properties (pellet resintering, pellet cracking, porosity)
- Cycle Exposure
- Change in fuel rod code to code other than RODEX2

The introduction of M5 cladding changes the cladding type. Therefore, consistent with the approved EMF-2310(P)(A) methodology, the first application involving M5 cladding requires that a [

] for use with M5

cladding.

The qualification of the RODEX2-2A model is described separately in Section 4.0. Since the approved methodology specifically addresses the possibility for differing cladding types, a sample problem is not required in this report to quantify the impact of the change from Zircaloy to M5 cladding.

8.1.2 Statistical Setpoint/Transient Methodology for Westinghouse Type Reactors

The statistical setpoint/transient methodology as applied to Westinghouse type PWR's is described in EMF-92-081(P)(A). It is used to calculate trip setpoints and to verify trip systems and limiting conditions of operation. The methodology is not affected by the use of M5 cladding material. Most of the phenomena evaluated in the methodology are associated with cladding surface effects. The evaluation of the fuel rod power associated with centerline melting represents the only fuel rod internal effect that participates in the analysis. This evaluation is performed with RODEX2-2A and is functionally identical for the two cladding materials. The qualification of the RODEX2-2A code is described separately in Section 4.0.

8.1.3 Statistical Setpoint/Transient Methodology for Combustion Engineering Type Reactors

The statistical setpoint/transient methodology as applied to Combustion Engineering type PWRs is described in EMF-1961(P)(A). It is used for analyzing limiting conditions of operation, limiting safety system settings and transients for Combustion Engineering PWRs. The methodology is not affected by the use of M5 cladding material. Most of the phenomena evaluated in the methodology are associated with cladding surface effects. The evaluation of the fuel rod power

associated with centerline melting represents the only fuel rod internal effect that participates in the analysis. This evaluation is performed with RODEX2-2A and is functionally identical for the two cladding materials. The qualification of the RODEX2-2A code is described separately in Section 4.0.

8.2 ***Summary of Clad Related Models in Non-LOCA Methodology***

8.2.1 RODEX2-2A

The RODEX2-2A code is used [] to determine appropriate clad and fuel burnup dependent fuel rod parameters for input to the S-RELAP5 calculation for SRP Chapter 15 non-LOCA transient analyses. The statistical setpoint/transient methodologies use RODEX2-2A to perform the fuel burnup and centerline fuel temperature calculations to determine the fuel melt limit. As describe in Section 4.0, the cladding related models implemented in RODEX2-2A for M5 cladding are:

- Cladding Creep
- Cladding free growth (and Axial Elongation)
- Cladding Thermal Conductivity
- Oxide Thermal Conductivity
- Cladding Coefficient of Thermal Expansion
- Cladding Modulus of Elasticity
- Cladding Poisson's Ratio
- Cladding Emissivity
- Cladding Corrosion

Cladding surface roughness is another cladding related parameter that is specified in user input.

8.2.2 S-RELAP5

The S-RELAP5 code is used to perform SRP Chapter 15 non-LOCA transient calculations. It performs the system thermal-hydraulic calculation including the average core and limiting hot spot (hot rod) heat transfer. []

] as described in the SRP Chapter 15 non-LOCA transients topical report EMF-2310(P)(A).

While current SRP Chapter 15 non-LOCA transient calculations use [

], the SER for EMF-2310(P)(A) approved the use of the RODEX2 models incorporated in the S-RELAP5 code for SRP Chapter 15 non-LOCA transient calculations if desired. The cladding related models implemented in S-RELAP5 for M5 cladding that are relevant to SRP Chapter 15 non-LOCA transients if the second option is used are as follows and were described in Section 5.0:

- Cladding Thermal Conductivity
- Oxide Thermal Conductivity
- Cladding Specific Heat]
- Cladding Density
- Cladding Coefficient of Thermal Expansion
- Cladding Modulus of Elasticity
- Cladding Poisson's Ratio
- Cladding Emissivity

Cladding surface roughness is another cladding related parameter that is specified in user input.

8.3 *M5 Properties and Correlations Implemented in Non-LOCA Models*

8.3.1 Cladding Creep Correlation

M5 cladding creep for non-LOCA calculations is implemented in the rod burnup calculation as discussed in Section 4.1.1 in the RODEX2-2A code. Note that cladding creep is a burnup dependent parameter. The duration of an S-RELAP5 SRP Chapter 15 non-LOCA transient calculation is sufficiently short to hold burnup dependent parameters constant. Therefore, cladding creep is not calculated in the S-RELAP5 code.

8.3.2 Cladding Free Growth

M5 cladding free growth for non-LOCA calculations is implemented in the rod burnup calculation as discussed in Sections 4.1.2 and 4.3 in the RODEX2-2A code. Note that cladding free growth is a burnup dependent parameter. The duration of an S-RELAP5 SRP Chapter 15 non-LOCA

transient calculation is sufficiently short to hold burnup dependent parameters constant. Therefore, cladding free growth is not calculated in the S-RELAP5 code.

8.3.3 Cladding Thermal Conductivity

M5 cladding thermal conductivity for non-LOCA calculations is implemented as discussed in Section 4.1.3 and 5.1.3 in the RODEX2-2A and S-RELAP5 codes, respectively.

8.3.4 Cladding Oxide Thermal Conductivity

M5 cladding oxide thermal conductivity for non-LOCA calculations is implemented as discussed in Section 4.1.4 and 5.1.4 in the RODEX2-2A and S-RELAP5 codes, respectively.

8.3.5 Cladding Specific Heat

M5 cladding specific heat for non-LOCA calculations is implemented as discussed in Section 5.1.5 in the S-RELAP5 code for SRP Chapter 15 non-LOCA transient calculations. Note that cladding heat capacity is not used in the RODEX2-2A code and, therefore, the statistical setpoint/transient methodology. RODEX2-2A calculations assume quasi-steady thermal conditions for each burnup interval so specific heat is not required.

8.3.6 Cladding Density

M5 cladding density for non-LOCA calculations is implemented as discussed in Section 5.1.6 in the S-RELAP5 code for SRP Chapter 15 non-LOCA transient calculations. Note that cladding density is not used in the RODEX2-2A code and, therefore, the statistical setpoint/transient methodology. Density would be multiplied by the specific heat to provide a volumetric heat capacity. However, RODEX2-2A calculations assume quasi-steady thermal conditions for each burnup interval so heat capacity and density are not required.

8.3.7 Cladding Thermal Expansion

M5 cladding thermal expansion for non-LOCA calculations is implemented as discussed in Section 4.1.7 and 5.1.7 in the RODEX2-2A and S-RELAP5 codes, respectively.

8.3.8 Cladding Modulus of Elasticity

M5 cladding Young's modulus for non-LOCA calculations is implemented as discussed in Section 4.1.8 and 5.1.8 in the RODEX2-2A and S-RELAP5 codes, respectively.

8.3.9 Poisson's Ratio

M5 cladding Poisson's ratio for non-LOCA calculations is implemented as discussed in Section 4.1.9 and 5.1.9 in the RODEX2-2A and S-RELAP5 codes, respectively.

8.3.10 Cladding Emissivity

M5 cladding emissivity for non-LOCA calculations is implemented as discussed in Section 4.1.10 and 5.1.10 in the RODEX2-2A and S-RELAP5 codes, respectively.

8.3.11 Cladding Corrosion

M5 cladding corrosion for non-LOCA calculations is implemented in the burnup calculation as discussed in Section 4.1.11 in the RODEX2-2A code. The duration of an S-RELAP5 SRP Chapter 15 non-LOCA transient calculation is sufficiently short to hold burnup dependent parameters constant. Therefore, low temperature cladding corrosion is not calculated in the S-RELAP5 code.

8.3.12 Cladding Hydrogen Pick-up

M5 cladding Hydrogen pick-up for non-LOCA calculations is implemented in the burnup calculation as discussed in Section 4.1.12 in the RODEX2-2A code. The duration of an S-RELAP5 SRP Chapter 15 non-LOCA transient calculation is sufficiently short to hold burnup dependent parameters constant. Therefore, low temperature cladding Hydrogen pick-up is not calculated in the S-RELAP5 code.

8.3.13 Cladding Surface Roughness

Surface roughness is an input parameter that is more closely associated with the cladding manufacturing process than the cladding material type. Currently, as manufactured surface roughness is input to the RODEX2-2A code for cladding internal surface roughness. It is not anticipated that M5 rod external surface roughness will differ substantially from Zircaloy cladding. Therefore, the same external surface roughness for the thermal-hydraulic calculation performed by S-RELAP5 will be used for M5 as is currently used for Zircaloy cladding (5.0×10^{-6} ft for typical drawn tubing, Reference 48, Page A-23).

8.4 *M5 Setpoint Methodology Sample Problem*

The fuel rod power associated with centerline melting was evaluated for a typical Westinghouse fuel type using both Zircaloy and M5 cladding materials. All other input parameters were held equal between the two analyses to provide an indication of the effects of the M5 cladding material. The fuel rod power associated with centerline melting for M5 clad fuel was observed to be less than one percent higher than the fuel rod power associated with centerline melting for zircaloy clad fuel. This small difference is consistent with expectations.

9.0 References

1. BAW-10227(P)(A), *Evaluation of Advanced Cladding and Structural Material (M5) in PWR Reactor Fuel*, Framatome Cogema Fuels, February 2000.
2. BAW-10231P-A, *COPERNIC Fuel Rod Design Computer Code*, Framatome Cogema Fuels, April 2002.
3. EMF-92-116(P)(A) Revision 0, *Generic Mechanical Design Criteria for PWR Fuel Designs*, Siemens Power Corporation, February 1999.
4. EMF-2328(P)(A) Revision 0, *PWR Small Break LOCA Evaluation Model, S-RELAP5 Based*, Framatome ANP Richland, Inc., March 2001.
5. EMF-2310(P)(A) Revision 0, *SRP Chapter 15 Non-LOCA Methodology for Pressurized Water Reactors*, Framatome ANP Richland Inc., May 2001.
6. EMF-92-081(P)(A) Revision 1, *Statistical Setpoint/Transient Methodology for Westinghouse Type Reactors*, Siemens Power Corporation, February 2000.
7. EMF-1961(P)(A) Revision 0, *Statistical Setpoint/Transient Methodology for Combustion Engineering Type Reactors*, Siemens Power Corporation, July, 2000.
8. XN-NF-81-58(P)(A) Revision 2 and Supplements 1 and 2, *RODEX2 Fuel Rod Thermal-Mechanical Response Evaluation Model*, Exxon Nuclear Company, March 1984.
9. XN-NF-81-58(P)(A) Revision 2, Supplements 3 and 4, *RODEX2 Fuel Rod Thermal-Mechanical Response Evaluation Model*, Advanced Nuclear Fuels, June 1990.
10. XN-NF-82-06(P)(A) Revision 1, Supplements 2, 4, and 5, *Qualification of Exxon Nuclear Fuel for Extended Burnup*, Exxon Nuclear Company, October 1986.
11. ANF-88-133(P)(A) Supplement 1, *Qualification of Advanced Nuclear Fuels' PWR Design Methodology for Rod Burnups of 62 GWd/MTU*, Siemens Nuclear Power Corporation, December 1991.
12. XN-75-32(P)(A) Supplements 1 through 4, *Computational Procedure for Evaluating Fuel Rod Bowing*, Exxon Nuclear Company, October 1983 [base document not approved].
13. XN-NF-696(P)(A), *ENC's Solution to the NRC Sample Problems-PWR Fuel Assemblies Mechanical Response to Seismic and LOCA Events*, Exxon Nuclear Company, April 1986.
14. XN-76-47(P)(A), *Combined Seismic-LOCA Mechanical Evaluation for Exxon Nuclear 15x15 Reload Fuel for Westinghouse PWR's*, Exxon Nuclear Company, January 1982.
15. ANF-90-82(P)(A) Revision 1, Supplement 1, *Application of ANF Design Methodology for Fuel Assembly Reconstitution*, Siemens Power Corporation, May 1995.

16. XN-NF-79-56(P)(A) Revision 1, Supplement 1, *Gadolinia Fuel Properties for LWR Fuel Safety Evaluation*, Exxon Nuclear Company, November 1981.
17. XN-NF-85-92(P)(A), *Exxon Nuclear Uranium Dioxide/Gadolinia Irradiation Examination and Thermal Conductivity Results*, Exxon Nuclear Company, November 1986.
18. EMF-96-029(P)(A), *Reactor Analysis System for PWRs*, Vol. 1, *Methodology Description*, Vol. 2, *Benchmarking Results*, Siemens Power Corporation, January 1997.
19. XN-NF-82-21(P)(A) Revision 1, *Application of Exxon Nuclear Company PWR Thermal Margin Methodology to Mixed Core Configurations*, Exxon Nuclear Company, September 1983.
20. XN-75-21(P)(A) Revision 2, *XCOBRA-IIIC: A Computer Code to Determine the Distribution of Coolant During Steady State and Transient Core Operation*, Exxon Nuclear Company, January 1986.
21. XN-NF-78-44(NP)(A), *A Generic Analysis of the Control Rod Ejection Transient for Pressurized Water Reactors*, Exxon Nuclear Company, October 1983.
22. EMF-92-153(P)(A), Supplement 1, *HTP: Departure from Nucleate Boiling Correlation for High Thermal Performance Fuel*, Siemens Power Corporation, March 1994.
23. EMF-2087(P)(A), *SEM/PWR-98: ECCS Evaluation Model for PWR LBLOCA Application*, Siemens Power Corporation, June 1999.
24. XN-75-41(A) Vols. I, II, Vol. II Appendices, and Vol. III Revision 2, and Supplements 1, 2, 3, 4, and 5 Revision 1, and Supplements 6 and 7, *Exxon Nuclear Company WREM-Based Generic PWR ECCS Evaluation Model*, Exxon Nuclear Company, February 1986.
25. XN-76-27(A) Supplements 1 and 2, *Exxon Nuclear Company WREM-Based Generic PWR ECCS Evaluation Model Update ENC-WREM-II*, Exxon Nuclear Company, March 1977.
26. XN-76-44(A), *Revised Nucleate Boiling Lockout for ENC WREM-Based ECCS Evaluation Models*, Exxon Nuclear Company, February 1977.
27. XN-CC-39(A) Revision 1, *ICECON: A Computer Program Used to Calculate Containment Back Pressure for LOCA Analysis Including Ice Condenser Plants*, Exxon Nuclear Company, October 1978.
28. XN-NF-78-30(A) Amendment 1, *Exxon Nuclear Company WREM-Based Generic PWR ECCS Evaluation Model Update ENC WREM-IIA Responses to NRC Request for Additional Information*, Exxon Nuclear Company, May 1979.
29. XN-NF-82-20(P)(A) Revision 1, Supplement 2, *Exxon Nuclear Company Evaluation Model EXEM/PWR ECCS Model Updates*, Exxon Nuclear Company, February 1985.

30. XN-NF-82-20(P)(A) Revision 1, Supplements 1, 3 and 4, *Exxon Nuclear Company Evaluation Model EXEM/PWR ECCS Model Updates*, Advanced Nuclear Fuels Corporation, January 1990.
31. XN-NF-82-20(P)(A) Revision 1, Supplement 6, *EXEM/PWR Large Break LOCA ECCS Model Updates*, Siemens Power Corporation, June 1998.
32. XN-NF-85-16(P)(A) Vol. 1 Supplements 1, 2 and 3; and Vol. 2, Revision 1 Supplement 1, *PWR 17x17 Fuel Cooling Test Program*, Advanced Nuclear Fuels Corporation, February 1990.
33. XN-NF-85-105(P)(A) Supplement 1, *Scaling of FCTF Based Reflood Heat Transfer Correlation for Other Bundle Designs*, Advanced Nuclear Fuels Corporation, January 1990.
34. XN-NF-82-07(P)(A) Revision 1, *Exxon Nuclear Company ECCS Cladding Swelling and Rupture Model*, Exxon Nuclear Company, November 1982.
35. EMF-2103(P), *Realistic Large Break LOCA Methodology for Pressurized Water Reactors*, Framatome ANP, Inc. [currently under review by the NRC].
36. ANF-90-145(P)(A) Vol. I and II, Supplement 1, *RODEX3 Fuel Rod Thermal-Mechanical Response Evaluation Model*, Vol. I, *Theoretical Model*, Vol. II, *Thermal and Gas Release Assessments*, Advanced Nuclear Fuels, April 1996.
37. ANF-88-054(P)(A), *PDC-3 Advanced Nuclear Fuels Corporation Power Distribution Control for Pressurized Water Reactors and Application of PDC-3 to H. B. Robinson Unit 2*, Advanced Nuclear Fuels Corporation, October 1990.
38. XN-75-27(P)(A) Supplement 5, *Exxon Nuclear Neutronics Design Methods for Pressurized Water Reactors*, Exxon Nuclear Company, February 1987.
39. XN-CC-32(P)(A), *XTRAN-PWR: A Computer Code for the Calculation of Rapid Transients in Pressurized Water Reactors with Moderator and Fuel Temperature Feedback*, Exxon Nuclear Company, September 1976.
40. E. V. Murphy and F. Havelock, "Emissivity of Zirconium Alloys in Air in the Temperature 100 - 400°C," *Journal of Nuclear Material* 60, 1976, pp. 167-176.
41. EMF-2100(P) Revision 6, *S-RELAP5 Models and Correlation Code Manual*, Framatome ANP Inc., August 2002.
42. L. Baker and L. C. Just, *Studies of Metal-Water Reactions at High Temperature: III. Experimental and Theoretical Studies of Zirconium-Water Reaction*, ANL-6548, 1962.
43. BAW-10227(P)(A) Enclosure 1, *Evaluation of Advanced Cladding and Structural Material (M5) in PWR Reactor Fuel*, Framatome Cogema Fuels, February 2000.
44. XN-76-27(A), *Exxon Nuclear Company WREM-based Generic PWR ECCS Evaluation Model Update ENC-WREM-11*, Exxon Nuclear Company, March 1977.

45. *Standard Review Plan for the Review of Safety Analysis Reports for Nuclear Power Plants*, NUREG-0800, 1st ed. November 1975, 2nd ed. March 1980, and 3rd ed. July 1981, U.S. Nuclear Regulatory Commission.
46. *ASME Boiler and Pressure Vessel Code*, Section III, Division 1, Article III-2000, Design Stress Intensity Values for Class 1 Components, 1977.
47. W. J. O'Donnell and B. F. Langer, "Fatigue Design Bases for Zircaloy Components," *Nuclear Science and Engineering*, Vol. 20, January 1964.
48. *Flow of Fluids Through Valves, Fittings, and Pipes*, Technical Paper NO. 410, Crane Company, 1988.

Distribution

Controlled Distribution

V. I. Arimescu, 31
M. R. Billaux, 31
C. A. Brown, 31
K. E. Carlson, 18
H. Chow, 18
K. M. Duggan, 31
B. M. Dunn, OF53
M. M. Giles, 18
R. L. Harne, OF12
P. J. Henningson, OF12
R. P. Martin, OF53
A. B. Meginnis, 18
T. E. Miles, CN70
J. C. Morris, 31
S.-H. Shann, 31
M. H. Smith, 31
J. H. Strumpell, CN70
D. A. Wesley, OF12
G. T. Williams, CN70

E-Mail Notification

D. M. Brown
R. E. Collingham
J. J. Cudlin
D. J. Gale
J. S. Holm
T. R. Lindquist
J. F. Mallay
J. R. Tandy